CHALMERS
UNIVERSITY OF TECHNOLOGY

Chemical-looping gasification for the production of aviation fuel with negative emissions:
Full chain process modeling and techno-economic analysis

Mohammad Shahrivar
Muhammad Nauman Saeed

DEPARTMENT OF SPACE, EARTH AND ENVIRONMENT

CHALMERS UNIVERSITY OF TECHNOLOGY

Gothenburg, Sweden 2022

www.chalmers.se

Contents

Abbreviations

AR	Air Reactor
ASU	Air Separation Unit
ATR	Autothermal Reformer
BFB	Bubbling Fluidized-Bed
BOP	Balance of Plant costs
BtL	Biomass to Liquid Fuel
CCS	Carbon Capture and Storage
CE	Chemical Efficiency
CEPCI	Chemical Engineering Plant Cost Index
CFB	Circulating Fluidized-Bed
CGE	Cold Gas Efficiency
CI	Conventional Inert
CLC	Chemical Looping Combustion
CLG	Chemical Looping Gasification
CRF	Capital Recovery Factor
d.b	Dry Basis
DH	District Heating
ESPs	Electrostatic precipitators
FR	Fuel Reactor
FT	Fischer-Tropsch
GHG	Greenhouse Gases
H2/CO	Hydrogen to carbon monoxide ratio based on number of moles
HHV	High Heating Value
HTFT	High-Temperature Fischer-Tropsch
IC	Indirect Costs
IDC	Interest During Construction
IPCC	Intergovernmental Panel on Climate Change
LCA	Life Cycle Assessment
LD	Linz-Donawitz
LHV	Low Heating Value
LTFT	Low-Temperature Fischer-Tropsch
MDEA	Methyl Diethanolamine
NC	Non-Conventional
O&M	Operation and Maintenance
OC	Oxygen Carrier
OLGA	Oil-based Gas Washing Absorber
PR-BM	Peng-Robinson equation of state with Boston-Mathias modifications
R&D	Research and Development
RME	Rapeseed Methyl Ester
S/B	Steam to biomass ratio based on mass
TEA	Techno-economic Analysis
TEM	Techno-economic modelling
TPC	Total Plant Cost
TPI	Total Plant Investment
WGS	Water Gas Shift

1 Abstract

The greenhouse gases from the conversion of fossil fuels are the main culprits for the increase in the planet's temperature which is reflected in the global warming context. The aviation sector is more dependent on fossil fuels as there is less possibility to find a viable alternative for fuel requirements for this sector. Chemical Looping Gasification with biomass as a fuel combined with downstream Fischer-Tropsch (FT) synthesis for aviation fuel production is a possible way to decarbonize transportation sectors like aviation. Chemical Looping Gasification (CLG) is like indirect gasification in a circulating fluidized bed, except that instead of inert bed material, particles containing metal-oxides, called oxygen carriers (OCs) are used as the bed material. CLG process has advantage of unnecessary use of an expensive and energy-intensive air separation unit (ASU). Also, due to the presence of a more oxidizing environment in CLG and the catalysing property of OC, the tar yield drops substantially resulting in improved syngas yield and better biomass to syngas conversion compared to the conventional gasification processes. Moreover, all produced CO_2 is concentrated in the fuel reactor, with no or limited emissions from the air reactor. This means that it could be a very good process for combined fuel production and capture of CO_2, something which would result in net-negative emissions.

The study is based on modeling the full chain process of biomass to liquid fuel (BtL) using Aspen Plus software. The model is designed for a gasifier load of around 80 MW_{th} and includes drying of biomass followed by a CLG unit using different oxygen carriers (LD slag and Ilmenite). The circulation rate of an oxygen carrier is adjusted to achieve the desired autothermal CLG operation with temperature of 935^{o}C in the fuel reactor (FR). The resulting syngas from CLG goes through syngas cleaning and conditioning units to meet the requirements for FT synthesis. The steam to biomass ratio is adjusted to 0.7 to achieve an H_2/CO ratio of 2.1 before the FT reactor. In the FT reactor with cobalt as a catalyst and at temperature of 220^{o}C, the syngas gets converted into hydrocarbons with carbon numbers ranging from 1 to 40 using the Anderson-Schulz-Flory distribution. Since the aim of the model is to produce aviation fuel, the FT synthesis process combined with a reformer in the recycle loop is adjusted for maximizing the yield of paraffin with carbon numbers ranging from 8 to 16.

Based on the optimized model, the clean syngas after syngas cleaning units has an energy content of 8.68 MJ/Nm^3 (LHV basis) with a cold-gas efficiency of 77.86 %. FT synthesis model with a reformer estimates an FT crude production of around 647 bbl/day with 154 kilo-tonne of CO_2 captured every year and conversion efficiency of biomass to FT-crude of 38.98 %. The calculated levelized cost of fuel (LCOF) is 35.19 $ per GJ of FT crude, with an annual plant profit (cash inflow) of 11.09 M$ and a payback period of 11.56 years for the initial investment.

2 Introduction

The greenhouse gases generated from conversion of fossil fuels are the primary cause of increase in the planet's temperature which is reflected in the global warming context. The greenhouse gases trap heat and make the planet warmer which has been progressing for the last 150 years at an accelerated rate [1]. Because fossil fuels account for around 80% of all global energy sources, replacing them with energy-efficiency measures or renewables by 2050 (as per the Paris Agreement) would be a monumental task. Solar or wind-generated energy, as well as nuclear power, are expected to replace a significant amount of fossil fuels. However, there will still be several situations where renewable carbon will be required. Aviation, long-distance transportation, and heavy haulage in rural regions, as well as diverse commodities and chemicals, are among them [2]. The share of the carbon dioxide (CO2) emission from the transportation sector is around one-fifth of the total CO2 emissions in the world. The transportation sector includes vehicles, trains, aviation, and marine where the aviation sector accounts for 11.6 % of the total transport emissions [3] In 2017, direct aviation emissions accounted for 3.8 % of overall CO2 emissions in the EU. Aviation accounts for 13.9 % of all transportation-related emissions, making it the second-largest source of GHG emissions after road transport. The European Green Deal calls for a 90 % reduction in transport emissions by 2050 to attain climate neutrality (compared to 1990-levels); therefore, the aviation industry will also have to contribute to the reduction [4].

The Paris Agreement established that the global temperature rise should be kept far below 2^{o}C, ideally it should be below 1.5^{o}C, over pre-industrial levels [5]. According to the Intergovernmental Panel on Climate Change (IPCC), achieving the 1.5^{o}C target will need global CO_2 emissions of little under 9 Gt CO_2/year by 2060 and net-zero CO2 emissions by 2100 [6]. To reach these targets a shift from fossil fuel-based products toward more sustainable fuels with carbon capture and storage is needed [7]. High energy prices, rising energy imports, prospective on future CO2 taxes, concerns about the security of petroleum supply, and a growing awareness of fossil fuels' environmental repercussions have sparked interest in alternative fuels. Biomass, unlike other renewable energy sources, may be turned directly into liquid fuels, known as "biofuels," to assist in meeting transportation fuel demands. The GHG emission from the combustion of biofuels will not add to CO2 in the atmosphere as the same amount of CO_2 will be consumed during the production of the biomass [1]. The present fossil fuel consumption rate and its dependency of the energy sector showed that the CO_2 budget that is essential to keep the target of global rise in temperature below 1.5^{o}C is going to be finished by the year 2028. This indicates the negative emission is essential to comply with this target [7]. The aviation fuel production from sustainable biomass with the inherent CO_2 capture technology will help in the reduction of CO2 emissions from the power sector as well the biofuel combustion sector. With the novel technology, chemical looping gasification (CLG), negative emission can be achieved together with fuel production and is hence aligned with the target of keeping increase in global average temperature below 1.5^{o}C [7][8].

This thesis aims to evaluate and optimize the full chain process of bio-aviation fuel production for technical and economic indicators using Ilmenite and LD slag as oxygen carriers for different process configurations at different operating conditions with the help of Aspen Plus process simulation tool. The process scheme is divided into different process units as given in Figure 2.1.

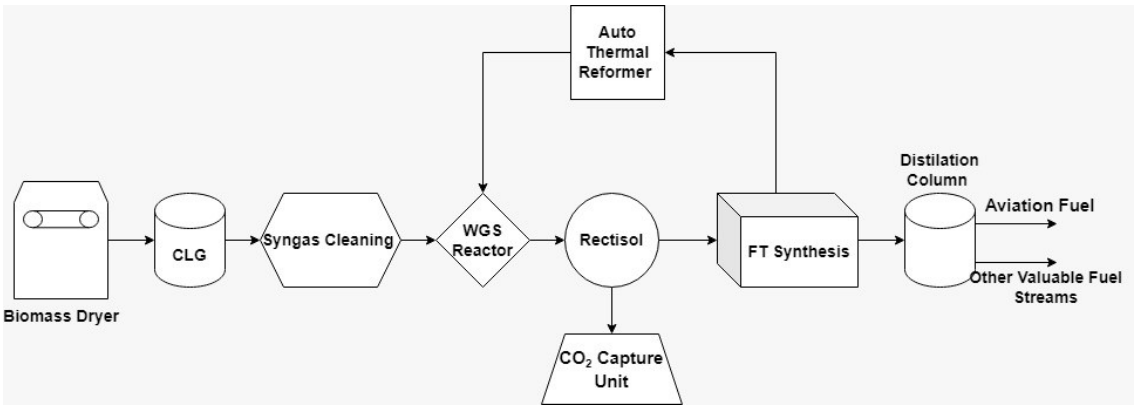

Figure 2.1 Full chain process model

The process includes the conversion of biomass energy using a Fluidized Bed Conversion (FBC) technology. As per the IEA report, Fluidized beds offers several advantages over pulverized fuel combustion/gasification, notably low NO_x emissions, in-process capture of SO_2, and the ability to burn a wide range of low-grade and potentially difficult fuels (including waste and biomass), as well as mixed fuels [9]. The fluidized bed reactors are mainly divided in two types: Atmospheric Bubbling Fluidized-Bed (BFB) and Atmospheric Circulating Fluidized-Bed (CFB). BFB is appropriate for low-fuel-ratio and/or low-heating-value fuels, such as biomass or garbage. CFB, on the other hand, is appropriate for fuels with a high fuel ratio. By supplying fluidizing agent from the furnace bottom, bed materials filled into the furnace are fluidized. Fuels are supplied into the furnace, which is kept at a constant temperature and gasified in the fluidized bed [9]. The thermal conversion (gasification) of the biomass or other carbon-based material always involves drying, pyrolysis, gasification, combustion, and reduction. After biomass conversion, the product gases can be used later in the chemical reactors and turned into hydrocarbon fuels. Gasification produces a minor amount of heat and a gaseous fuel made up of carbon monoxide (CO), hydrogen (H2), methane (CH4), CO2, and water vapor (H2O). There is also a large quantity of nitrogen present, depending on the gasifying agent (air, carbon dioxide, or steam) [10].

Furthermore, fluidized bed gasification can be divided into two categories - direct and indirect. Indirect fluidized bed gasification becomes more popular in some applications due to its advantage compared to direct fluidized bed gasification. The gases produced from the indirect fluidized beds are N_2 free due to the separation of the combustion and gasification reactors. However, the CO2 will be emitted from the combustion reactor and need a downstream CO2 capture unit to capture and store carbon dioxide [11]. This extra unit has immense consequences on the energy and economic point of view of the plant and needs to be taken into consideration for the environmental aspect of the plant [12].

The chemical looping gasification of biomass is a genuine alternative that is based on indirect gasification which increases the energy efficiency and simplifies the process of creating renewable hydrogen, synthetic fuels, or chemicals while having the benefit of confining the CO_2 emission. CLG eliminates the requirement for air separation equipment by achieving inherent air separation through the utilization of oxygen carriers [13]. The CLG system is made

up of two fluidized bed reactors that are linked together: an Air Reactor (AR) and a Fuel Reactor (FR). Metal oxide particles, which function as oxygen transporters, transport oxygen between the two reactors [14]. The oxygen carrier will oxidize in the AR and then be reduced in the FR as it is shown in Figure 2.2.

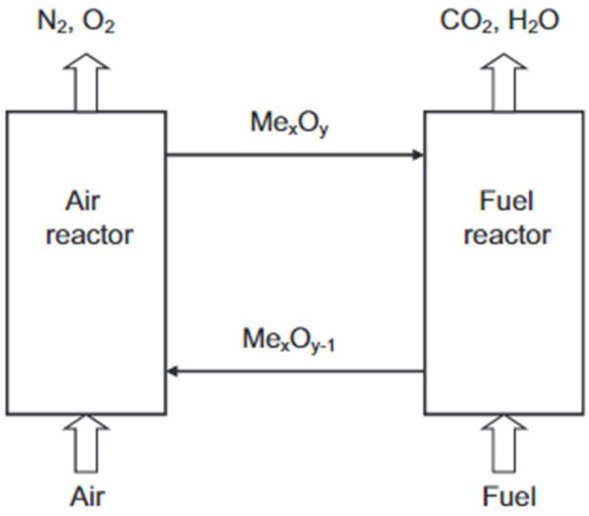

Figure 2.2 CLG process concept [14]

The oxygen carrier provides some advantages compared to the inert bed materials such as:

- More oxidizing environment in the fuel reactor due to higher partial pressure of CO_2 and H_2O than in indirect gasification.
- Catalytic characteristics of the oxygen carrier result in higher syngas yield and low tar content in the syngas (cleaner syngas).
- Expensive and energy-intensive Air Separation Unit (ASU) not needed.

Ishida et al. (1986) first used the term "chemical looping" to describe the method in which a metal oxide is employed as an oxygen transport medium to carry out a redox reaction scheme to boost exergy efficiency in power production [15]. Tar formation is problematic in biomass conversion and gasification, however, studies on chemical looping gasification by Mendiara et al (2013) indicate that the tar level is reduced by around 2.4 percent per degree Celsius in the range 880-915 ^oC [16], [17]. It is also stated in the paper by Zheng and Huang that $NiFe_2O_4$ shows a dual role as an oxidation-catalyst for toluene reduction and considerably enhances toluene conversion into carbon and H_2 [16], [18]. An experimental study on biomass gasification using chemical-looping with nickel-based oxygen carrier in a 25 kWth reactor has been done by Ge Huijun et al (2015) which showed the enhancement of biomass gasification and syngas yield by introduction of CaO into the oxygen carrier[16], [19]. The same study has also been done by Sozen et al. (2015) for different oxygen carriers which showed higher carbon conversion, gasification efficiency, and H2 production at 870^oC [20]. However, the use of Ni-based materials in fluidized beds maybe associated with high cost of environmental issues. Recent experimental investigations on chemical looping gasification with the by-product LD slag and Fe-Ti ore Ilmenite as oxygen carriers have been carried out by Condori. In these studies, the oxygen carrier performances were reported under different operational conditions and gasification agents. The results indicate that the processes have high biomass

conversions and high carbon conversion efficiency with sufficient syngas yield for autothermal operation and suggested the Fe-based oxygen carriers LD-slag and Ilmenite as suitable oxygen carriers for chemical looping gasification [21], [22].

The syngas produced in CLG unit goes through the syngas cleaning section that removes the ashes, tar, hydrogen sulfide, and CO_2 and prepares the syngas to be suitable for sending to the fuel production unit. The Rapeseed Methyl Ester (RME) scrubber and bag filter are used for the removal of the tar and ashes from the syngas, respectively. Later the syngas passes through an amine absorber to remove CO_2, hydrogen sulfide, and other gas contaminants from the syngas. The syngas is also conditioned using a water gas shift reactor to get the desired H_2/CO molar ratio required for the Fischer Tropsch (FT) synthesis. There is an additional acid gas removal unit (Rectisol unit) after the Water Gas Shift (WGS) reactor to remove any CO_2 produced in the WGS unit before the syngas stream enters the FT reactor. Fisher-Tropsch synthesis can be defined as a process that converts synthesis gas containing hydrogen and carbon monoxide to hydrocarbon products [23]. The process requires a specific condition of syngas before the FT reactor which makes it vital to condition the syngas. FT synthesis is a highly exothermic process that uses Iron or Cobalt-based catalysts to convert the syngas to hydrocarbons. Fisher-Tropsch synthesis can be either low-temperature Fisher-Tropsch (LTFT) or high-temperature Fisher-Tropsch (HTFT) depending on the fuel that is aimed to be produced. LTFT results in significantly longer hydrocarbon chains whereas HTFT produces mostly shorter hydrocarbons [24]. Therefore, in this work, the LTFT reactor has been modeled to produce aviation fuel. The FT crude from the FT reactor contains hydrocarbons ranging from 1 to 40 in carbon number. The lighter hydrocarbons in the gaseous phase are sent to an auto thermal reformer to convert them back to syngas before mixing with the clean syngas from the syngas cleaning unit, whereas the heavier hydrocarbons are sent to an atmospheric distillation column. The atmospheric distillation column is used to extract different fractions such as natural gas, gasoline, aviation fuel, diesel, and wax with carbon numbers ranging from 1 to 3, 4 to 7, 8 to 16, 17 to 22, and greater than 22, respectively.

Biomass to liquid fuel (BTL) is not a contemporary process and is well known from the 20th century when Germany developed the process to produce liquid fuel from their coal sources [25]. A study by Hamelinck in 2003 on the production of transport fuel from biomass indicated that the BTL production is expensive compared with other conventional methods of fuel production [26]. The paper suggested that the technology will become economically feasible when the crude oil price increases dramatically, or the CO2 tax increases making green FT products more compatible in the market. Furthermore, the techno-economic feasibility for the production of sustainable aviation fuel has been investigated by Spyridon Achinas, the results of which concluded that no industrial technique could compete with traditional jet fuel costs economically; policy, on the other hand, could help the bio-jet fuel sector by investing in research to cut manufacturing costs [27]. The study also concluded that the potential of biomass feedstock for efficient manufacturing is still untapped, and the sustainability of bio-jet fuel is limited. Ioanna Dimitriou et al. (2018) reported a techno-economic and uncertainty analysis of transport fuel production from the BTL process and suggested that there is a realistic probability (8–14%) of transport fuel production based on Fischer-Tropsch synthesis reaching conventional fuel costs; with reasonable tax incentives, this probability might go up to 50 percent [28].

In this thesis, a techno-economic comparison of Biomass to Liquid (BtL) process for different oxygen carriers, configurations and conditions is conducted to compare the effect of different parameters on the economic feasibility of the overall process.

The cost of all components was calculated based on literature. These costs were scaled to the model size based on the respective scaling units. The capital costs of the equipment were then adjusted with the CEPCI indices for inflation effects to calculate the Total Plant Cost (TPC). Later, Interest During Construction (IDC) was also included as a percentage of the TPC to get the Total Plant Investment (TPI). An overhead cost was added to the TPI to compensate for capital costs of small equipment such as heat exchangers and some small pumps and compressors which are needed to adjust for the pressure losses. The prices for fuel products, electricity, and district heating are assumed based on the literature and present value in the market.

3 Literature (background)

The chemical processes involved in converting biomass residues to aviation fuel can be collectively referred to as 'Biomass to Liquid (BtL).' In this chapter, a literature review of all the components and processes involved in BtL has been done.

3.1 Fuel (biomass)

The planet earth has a natural carbon cycle that sequesters carbon into nature. It can be saved either in the form of life in oceans or land as biomass or the human body. The biomass, more specifically the plants, uses the atmosphere CO2 and sequesters some portion of that carbon in the plant's chunk and some part in the soil. The energy for this carbon usage comes directly from the sun for the plant's photosynthesis process [29]. Photosynthesis is a process through which plants and other organisms transform solar energy into chemical energy that may be utilized to drive the organism's activities. Usage of biomass for energy means entering this natural cycle which makes the energy from this source carbon neutral. If this fuel is used for aviation fuel production and carbon is captured and stored a negative emission can be achieved. The use of biogenic fuel sources conserves the environment, lowers the need for petroleum, and offers rural areas economic opportunity. Furthermore, BtL made from cellulosic wastes and residues significantly reduce greenhouse gas emissions when compared to conventional biofuels made from rapeseed or wheat, which are linked to indirect emissions related to land use change [30].

Biomass is recognized to be mostly composed of three primary components (hemicellulose, cellulose, and lignin), with a trace quantity of extractives and minerals. On a dry basis, cellulose, hemicellulose, and lignin typically account for 40-60, 20-40, and 10-25 weight percent of biomass materials, respectively [31]. The ultimate analysis of biomass consists of carbon (C), hydrogen (H), oxygen (O), nitrogen (N), and a negligible proportion of sulfur (S). Agricultural residues, crop residues, forestry, parks and gardens, garbage, and other biomass feedstocks are examples of biomass feedstock suitable for energy applications.

While much of the focus has been on biomass for District Heating (DH), there is also a lot of interest in biomass availability and exploitation for other purposes. Sweden contributes around 10% of the sawn wood, pulp, and paper marketed on the worldwide market while having just 1% of the world's commercial forest areas. The forest residue is a reliable source of biomass in Nordic countries' geographical environments. The forest offers not just sawn wood and pulpwood, but also forest thinning, logging leftovers, and most of the fore undergrowth utilized in bioenergy. These waste products are utilized to make biofuel for heating and energy generation, as well as pellets for heating and liquid biofuels such as diesel, and aviation fuel [32] The use of biomass as fuel needs some consideration regarding the inherits of such fuels which were explained in C. Wang et al. [33].

The calorific value of biomass is a measure of the energy chemically bound in it, which is converted into heat energy during the combustion process. The most essential attribute of a fuel that affects its energy worth is its calorific value. The heat capacity of biomass fuel can be experimentally investigated or computed from the findings of its ultimate and/or proximate analysis. For combustion, it is important to know the ash content in the biomass

because the melting point of ash is lower compared to the combustion temperature due to its alkaline content, resulting in fouling and slagging. However, since the gasification temperatures are not as high as that of combustion, melting of ashes is not a problem in general [34]. It is also important to know the chlorine and alkali content of the biomass since high amounts of chlorines and alkali can lead to corrosion.

The biomass heating value can be reported based on LHV or HHV, which can be either based on dry or wet. Typical biomass has high moisture which affects the fuel heating value (on average 30%) compared with fossil-based fuels for example coke (6 %). The table below shows the ultimate and proximate analysis of the typical biomass in Nordic countries [35].

Table 3.1 Biomass composition

	Forest residue in Sweden	**Forest residue in Denmark**
HHV (MJ/kg d.b*)	20.67	20.54
Proximate analysis (wt. % d.b)		
Volatile Matter	79.3	74.1
Fixed Carbon	19.37	21.85
Ash	1.33	4.05
Ultimate analysis (wt. % d.b)		
C	51.3	51
H	6.1	5.8
O	0.4	0.9
N	40.85	38.21
S	0.02	0.04
ASH	1.33	4.05

**d.b. dry basis*

3.2 Feedstock logistics and Biomass pre-treatment

The availability of the fuel is an essential part of any conversion process which depends on the type of fuel and the conversion technology. The process of logistics can be divided into the fuel transport, storage, chipping, crushing, and drying. Any disturbance in the logistic process can cause an unforeseen shutdown of the plant; therefore, it is essential to have a reliable fuel handling process in aviation fuel production [36].

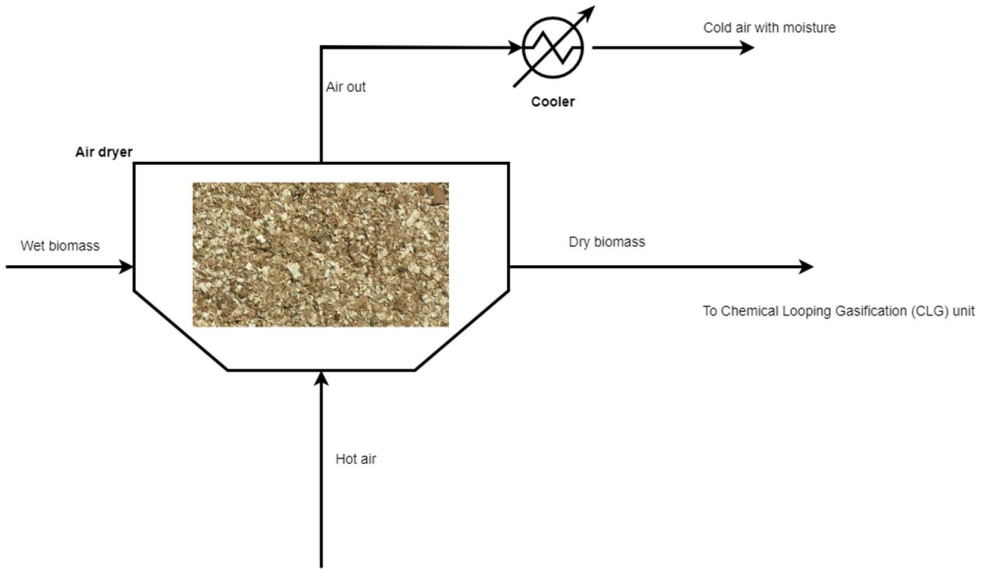

Figure 3.1 Biomass Drying Unit

According to Table 3.1, the energy content of the biomass is related to the moisture content of the feedstock. In this study, a forest residue is considered for the process which typically has 50 % moisture and LHV of 8-9 $\frac{MJ}{Kg}$. The pretreatment of the fuel such as drying is required to improve the syngas quality which will affect the thermal efficiency and the chemical efficiency of the plant [23]. Other physical pretreatment techniques for biomass intended as fuel for thermo-chemical conversion processes include torrefaction, pelletization and densification. These pretreatment methods employ heat to start chemical reactions that improve the properties of the biomass. In order to increase the quality of the biofuels produced and the economic viability of the pyrolysis and gasification processes, dry torrefaction (DT), a thermal pre-treatment procedure for biomass carried out at 200–300 C and low heating rates under inert air circumstances, advances the structure of the biomass. The fiber structure and tenacity of the biomass are altered during the torrefaction process, which may aid in lowering the activation energy for the pyrolysis and gasification processes [37]. Pelletizing biomass enables simple and affordable handling in addition to cost savings in transit and storage. Biomass pellets' regular shape and small size enable automated feeding with extremely precise calibration. The high density of pellets also enables efficient long-distance transportation and compact storage. Due to its high density and low moisture content during production, pellets have a very high combustion efficiency [38]. Mechanical densification and pyrolysis are the two major methods used to densify biomass. The process of mechanical densification requires applying pressure to the material. Pyrolysis is the process

of heating biomass without adding oxygen [39]. In this study, however, only a drying unit is considered and modelled in Aspen Plus. According to Hannula et al. (2016) fully drying the biomass is problematic due to challenges of energy efficiency, emissions, heat integration and dryer performance. In synthesis gas production, feedstocks must be dried to less than 30% moisture content, preferably to less than 15%, and in pyrolysis to less than 10% [36].

3.3 Biomass Gasification

Gasification is referred to as a thermo-chemical conversion process that converts carbon-containing fuels into a carbon monoxide (CO) and hydrogen-rich (H_2) gas mixture known as synthesis gas. Carbon dioxide (CO_2), nitrogen (N), water (H_2O), methane (CH_4), and tars are among the final products. The kind of process for introducing the fuel to the reactor, their feed ratios, process parameters, and the type of gasification reactor used all influence the specific composition of the final produced gas.

Different types of gasification reactors have been established previously but fluidized-bed reactors have been approved as a dependable and viable alternative for industrial large-scale biomass gasification [11]. Direct and indirect fluidized bed gasification are two main types of these kinds of reactors. The difference between direct and indirect is that in an indirect fluidized bed reactor the combustion and gasification reactors are separate while they are present in the same unit, which gives an advantage to N_2-free syngas products. The chemical looping gasification (CLG) is based on the same technology as the chemical looping combustion (CLC) where solids and gaseous fuels are fully oxidized in the Fuel Reactor (FR). The bed material in this technology is an oxygen carrier or a metal oxide particle which is reduced in a fuel reactor (FR) and oxidized in an air reactor (AR). The oxygen carrier provides enough oxygen requirement for combustion while removing direct contact between the air

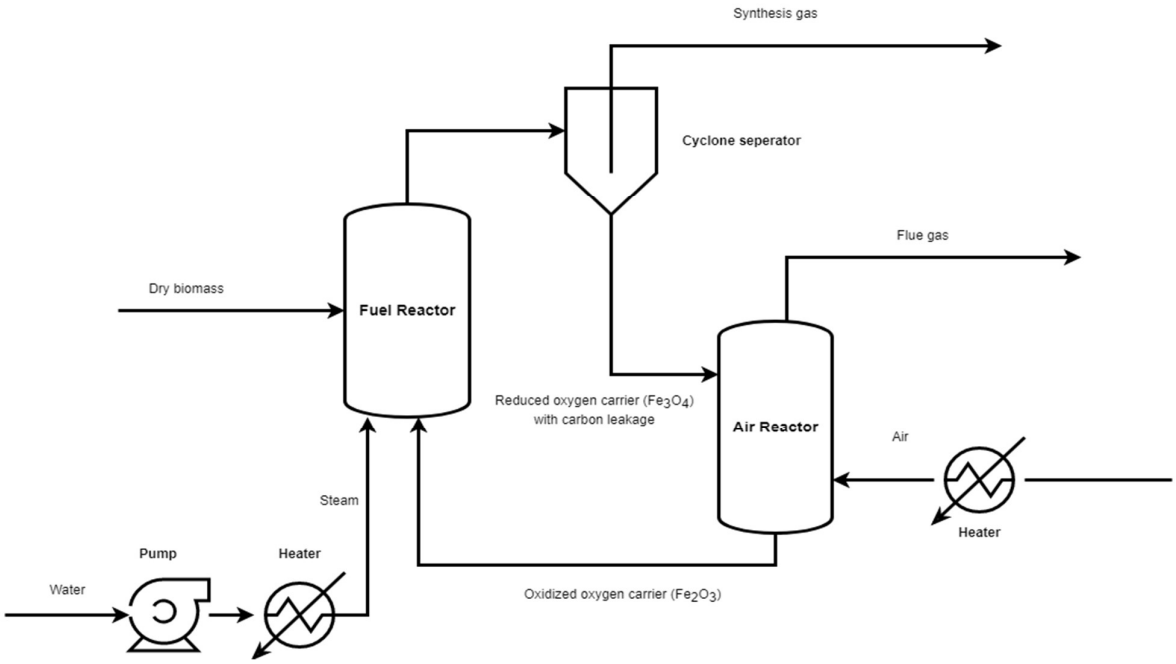

Figure 3.2 Chemical looping gasification flowchart

and fuel, therefore; the gaseous product from FR is mainly CO_2 and steam. The steam can be easily condensed to separate CO_2 from the stream. This reduces the energy requirement for the carbon capture unit as less electrical work is needed for compression in the carbon capture process [12]. Furthermore, the oxygen carrier will result in removing the need for air separation unit which improves the economic and energy penalty of the process. The same concept is used in the CLG while the aim is gasification of biomass in the fuel reactor rather than complete combustion. The fundamental goal of CLG is to create high-quality syngas by partially oxidizing the fuel in the FR. Nonetheless, in CLG, a part of the fuel will be oxidized to carbon dioxide and steam in addition to syngas CO and H_2 [40]. The sensible heat needed for the fuel conversion in the fuel reactor is obtained by the exothermic oxidation of oxygen carrier in the air reactor. In comparison to indirect gasification, no combustion of fuel is needed in the air reactor.

3.3.1 Chemical reactions for gasification

The reaction process in chemical looping gasification of biomass includes devolatilization, steam gasification of char, and gas-solid interactions involving volatile gases and oxygen carriers.

$$Biomass \rightarrow Char + Volatile\ gases(H_2 + CO + CO_2 + H_2O) + Tar \quad (1)$$

The gasification agent in the fuel reactor can be either steam or carbon dioxide. In this study, the source of the gasification agent is set to be Steam and the chemical formula for this reaction is illustrated below:

$$C + H_2O \rightleftharpoons CO + H_2 \quad (2)$$

The next reaction that is happening during biomass gasification is the Boudouard reaction in which carbon in presence of carbon dioxide will turn into carbon monoxide. The biomass gasification and the Boudouard reaction are exothermic

$$C + CO_2 \rightarrow 2CO \quad (3)$$

Two main reactions happen during gasification such as methane formation and water gas shift reaction both of which are endothermic reactions.

Methane formation:

$$C + 2H_2 \rightarrow CH_4 \quad (4)$$

Water-gas shift reaction:

$$CO + H_2O \rightarrow CO_2 + H_2 \quad (5)$$

The gasification process can be expressed based on a general formula that shows the combination of the steam gasification and water gas shift reaction as below:

$$\mathrm{C} + \alpha\, H_2\mathrm{O} \rightarrow (2 - \alpha)\,\mathrm{CO} + (\alpha - 1)\,\mathrm{CO_2} + \alpha\mathrm{H_2} \quad (6)$$

The α value is a mechanism factor that is determined experimentally for the gasification process and is proportional to the temperature. Studies show that by increasing the temperature, the α value will decrease. For instance, for the gasification process between 750 -900 Celsius the α value is reported as 1.5 – 1 respectively [41].

3.3.2 Chemical Looping Gasification

Chemical looping oxidation reactions need the use of metal oxide materials. The oxygen carriers give the necessary quantity of oxygen ions for hydrocarbon conversion and product synthesis during reduction. The depleted metal oxide oxygen carriers are supplied with molecular oxygen from the air during the oxidation stage, which also releases heat[42]. Oxygen carrier in the CLC unit for full oxidization of the volatiles is required, therefore; the OC should be chosen to have a higher reaction rate and maximum transport capacity. while in the CLG it is not required to fully oxidize the volatiles and control of the transport capacity is essential. The reactions in the fuel reactor for the Fe-based LD slag oxygen carrier are expected as below [43].

$$3Fe_2O_3 + H_2 \rightarrow 2Fe_3O_4 + H_2O \quad (7)$$

$$3Fe_2O_3 + CO \rightarrow 2Fe_3O_4 + CO_2 \quad (8)$$

$$12Fe_2O_3 + CH_4 \rightarrow 8Fe_3O_4 + CO_2 + 2H_2O \quad (9)$$

The transport capacity of an oxygen carrier is defined as the difference between the mass of the oxidized and reduced OC (including inert materials) divided by the mass of the oxidized oxygen carrier [44].

$$R_o = \frac{W_{oxidized} - W_{reduced}}{W_{oxidized}} \quad (3.1)$$

where $W_{oxidized}$ and $W_{reduced}$ are the mass flow rates of oxygen carriers entering and leaving the fuel reactor respectively.

There is no proper control of the oxygen carrier transport capacity. However, by varying the amount of inert material in the oxygen carrier, the oxygen transport can be increased or decreased. In the Air Reactor (AR), air flow can also be adjusted to not fully oxidize the metal oxide, as the result, the reduced metal oxides act as inert materials in the Fuel Reactor (FR), and the oxygen transport drops [45], [46]. In our model, we do not control the oxygen transport capacity, it is only a consequence of changing the Fuel Reactor (FR) temperature.

3.4 Syngas cleaning

The destination and product of any syngas that is produced from the gasification unit require syngas that is clean and pure from contaminates such as sulfur, NH3, tar, and ash. As a result, while gas cleanup processes are required, they have a significant influence on plant economics, as they can account for a significant amount of the entire capital and operating expenses. Even though raw syngas leaves the gasifier at a high temperature (around 935°C), traditional gas cleaning is usually done at a low temperature. The cost of the cooling

equipment, as well as the necessity to reheat the syngas before using them in the synthesis reactor, results in economic and thermodynamic penalties that reduce a gasification plant's efficiency. The cooling process can be used later for district heating and/or to reheat the syngas before the FT reactor [47].

3.4.1 Fly ash removal unit

The syngas exiting the fuel reactor will pass through a cyclone to separate the oxygen carrier from syngas and recirculate the oxygen carrier to AR. Cyclones, which can reach temperatures of over 1000 degrees Celsius, are one of the oldest and most widely used solids separation machines. They use centripetal acceleration to shorten the time it takes for tiny particles to settle due to gravity.

The cyclones are not sufficient for tiny particles in syngas therefore stronger equipment are needed for removing fly ash. Particles can also be removed from gas flows using electrical characteristics. Particles are charged by a strong electric field and then evacuated due to their electromagnetic characteristics. Electrostatic precipitators (ESPs) are often used in coal-fired power stations to remove fly ash at temperatures up to 200 degrees Celsius and have even been utilized at temperatures over 400 degrees Celsius [48].

3.4.2 Tar removal unit

Later in the process, wet scrubbers can remove tar and particle debris. Even though many tar compounds are insoluble in water, wet scrubbing lowers the gas temperature enough for many tarry vapors to condense as tiny particles that are easily absorbed by water droplets. Lighter class two and three tar components, such as phenol, stay in the vapor phase but are water-soluble enough to be absorbed by water droplets [48][47]. Oil-based gas washing (OLGA) is an absorber technology that is mainly designed for tar removal from gasification operation temperatures between 800-900 C [48], [49]. The tar composition transforms from a big multiple ring tar structure with high condensation points to thinner single or double ring tar elements with lower dew points as the temperature drops. Furthermore, the tar's composition will alter from non-polar components that are relatively stable to reactive polar components. For high-temperature gasifiers, rapeseed methyl ester (RME) can be used while for low-temperature gasifiers glycerol (preferred above RME and biodiesel) can be used [49]. Figure 3.3 shows the schematic for the ash and tar removal used in our model.

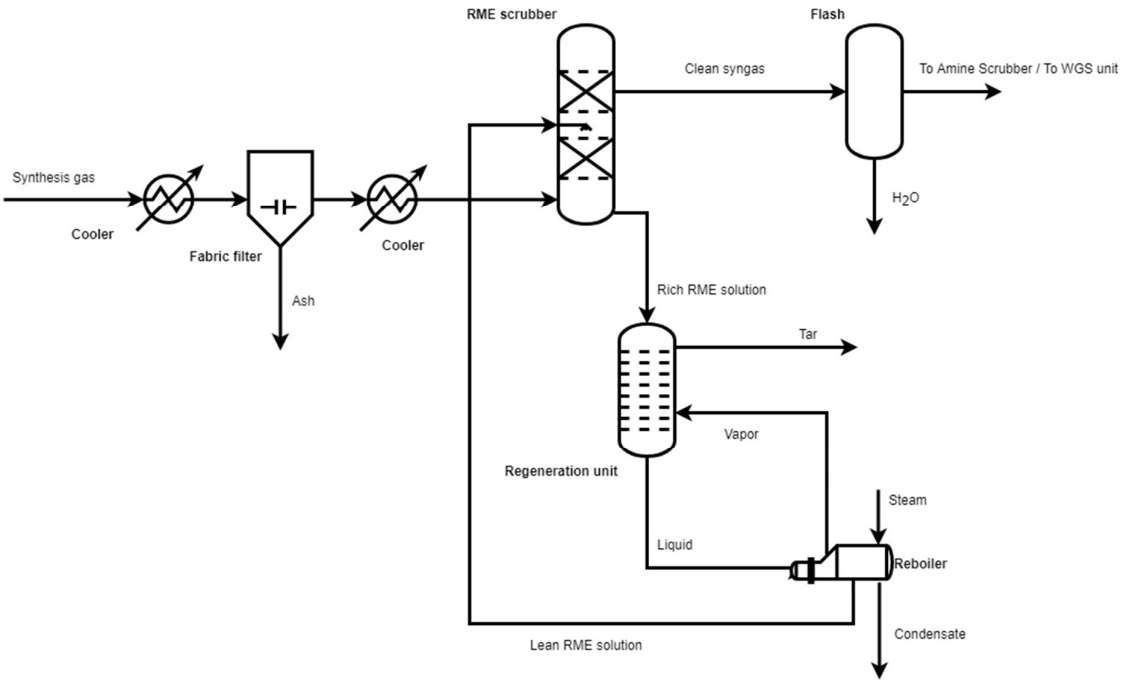

Figure 3.3 Ash and Tar removal units

The extremely polluted water from the wet scrubber enters a settling tank, where water-insoluble tar compounds are separated from the water, allowing the water to be recirculated back to the scrubber. The water-soluble tars eventually build up and decrease the wet scrubber's efficiency. Without biochemical and/or biological wastewater treatment, this effluent cannot be released into the environment [48].

3.4.3 Acid gas removal units

Low-temperature sulfur removal can be accomplished in a variety of ways. The most common solvent procedures are chemical, physical, or combination chemical/physical. Chemical redox processes, as well as biochemical reactions, are frequently used, particularly in sulfur recovery systems. A liquid solvent is used to form a weak chemical connection between an amine molecule and an acid gas, most frequently H_2S and CO_2. The downflowing amine solution absorbs hydrogen sulfide and carbon dioxide from the up flowing sour gas in the absorber, yielding a sweetened gas stream (a gas that is free of hydrogen sulfide and carbon dioxide) as a product and an amine solution rich in the absorbed acid gases [48]. Amines are classed as primary, secondary, or tertiary based on whether organic groups have replaced one, two, or three of the hydrogen atoms in ammonia.

R.R. Bottoms invented alkanolamines in 1930 for the absorption of acidic gases, which is one of the earliest industrial sulfur removal technologies. Other alkanolamines, such as the more frequently used mono ethanolamine (MEA), diethanolamine (DEA), and the newly popular methyl diethanolamine (MDEA, a tertiary amine), eventually superseded the first commercially accessible triethanolamine (TEA) [50].

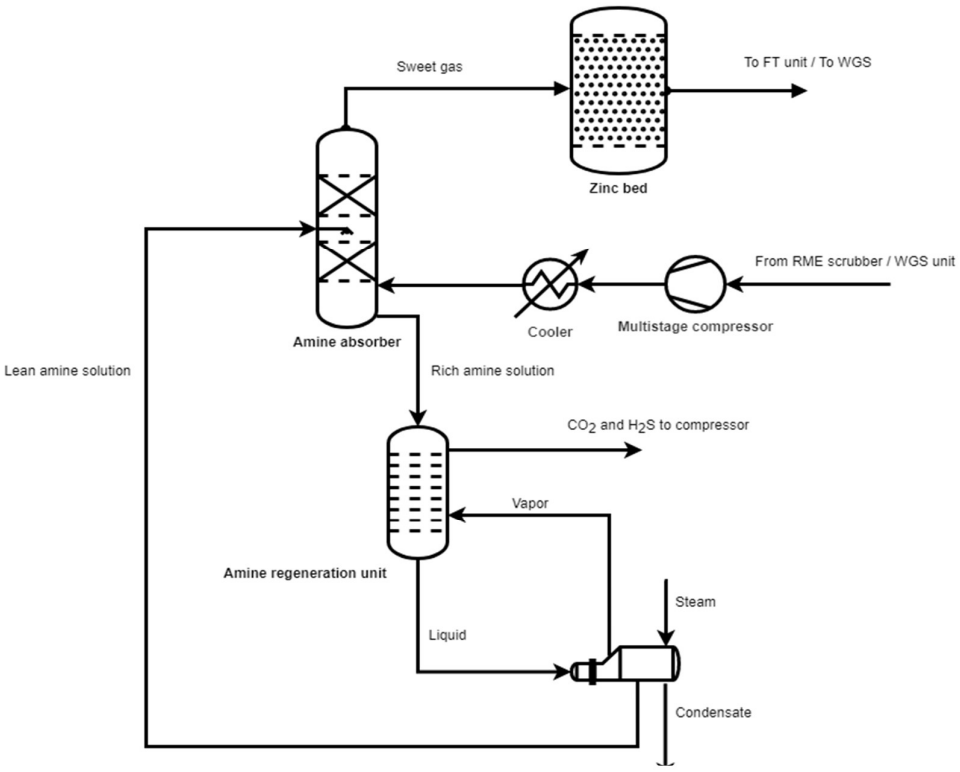

Figure 3.4 Amine Absorber

Because of its strong H_2S/CO_2 selectivity, stability against degradation, and low corrosivity, MDEA has become popular in the natural gas sector. MDEA units are used in a variety of applications all around the world.

The syngas is injected into the bottom of a trayed or packed tower and contacted with a lean, regenerated solvent counter currently. At the top of the tower, the treated gas, which is now free of acid gases, departs. The rich solvent, now laden with acid gases, is transferred to a stripping tower at the bottom of the absorption tower for regeneration [51]. Figure 3.4 shows the simplified scheme of the process along with a zinc oxide guard bed which removes traces of sulfur left in the syngas stream. The most popular adsorbent for removing H_2S from gas streams like natural gas or syngas is probably zinc oxide. Its quick intrinsic kinetics at moderate to high temperatures (200 – 450 °C) and strong stability in reducing environments contribute to its high capacity [52].

Another mature technology to remove acid gases from syngas is the Rectisol technology (Figure 3.5), which is the most widely used physical solvent gas treatment process in the world. Deep sulfur removal from synthesis gases, which are subsequently catalytically converted to Fischer Tropsch liquids, is its most typical use. The Rectisol process uses chilled methanol that can have a temperature as low as -70 degrees Celsius [51].

According to Kohl et al. [53] methanol has a low viscosity at these temperatures; thus, mass and heat transfer are not seriously affected, and the solvent's carrying capacity for both CO_2 and H_2S increases dramatically, much exceeding that of other physical solvents at their typical operating temperatures. With H_2S concentrations of typically 0.1 ppm and CO_2

concentrations of just a few ppm in the treated gas, these properties allow for very sharp separations [53].

Rectisol's strong selectivity for H_2S and COS is the process's key benefit over other technologies. Chilled methanol also absorbs HCN, NH_3, and iron- and nickel-carbonyls which is crucial for the downstream processes such as Fischer Tropsch Synthesis (FTS). However, Rectisol's complex system and the necessity to refrigerate the solvent are its principal drawbacks, resulting in expensive capital and operational expenses [51].

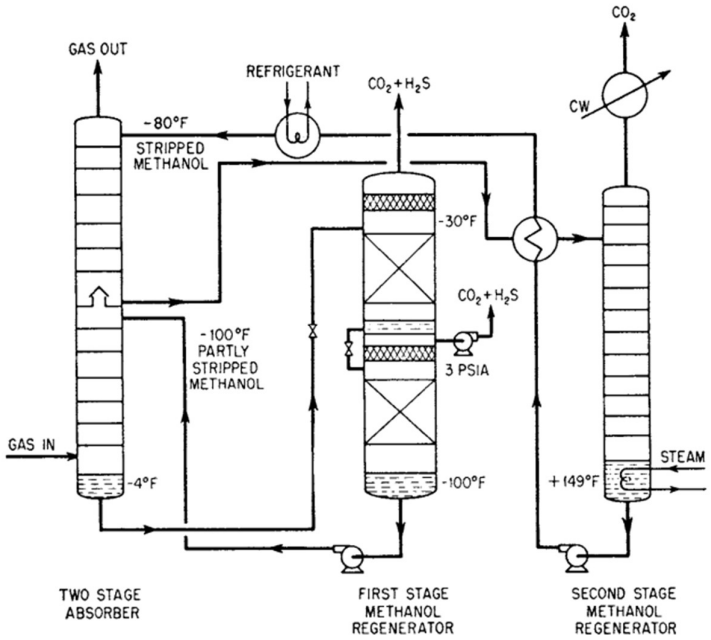

Figure 3.5 Rectisol process flow diagram [53]

The downstream process of BtL, which is the Fischer-Tropsch process, contains a catalyst that is sensitive to the contaminants present in the syngas produced from different biomass feed in the gasification process. The syngas cleaning should perform such that the limitation for the contaminants is achieved before entering the FT unit. Table 3.2 shows the maximum presence of the contaminants in the syngas that the catalyst can tolerate [54].

Table 3.2 Syngas purification for FT synthesis [39]

H_2S	$H_2S+COS+CS_2$ < 1 ppm
COS	
HCN	HCN + NH3 < 1 ppm
NH_3	
Alkalis	HF + HCl + HBr < 0.01 ppm
Halides	< 0.01 ppm

3.5 Water Gas Shift reactor

For optimum conversion, the syngas composition before the FT reactor must meet certain parameters, such as the H_2/CO ratio and syngas cleaning conditions as described in the previous section. H_2/CO ratio can be adjusted by the conditioning unit before the FT reactor. The specific ratio, which depends on product type and catalyst, will be controlled by the water-gas shift reactor. Water-gas shift reaction is an exothermic reaction that forms as below:

$$CO + H_2O \rightarrow CO_2 + H_2 \qquad \Delta H^0_{298} = -41 \text{ KJ mol}^{-1}$$

The water-gas shift reactor consists of three parts: high-temperature reactor, heat-exchanger, and low-temperature reactor as shown in Figure 3.6. These units are controlled such that the required H_2/CO ratio is achieved. The temperature is governing which direction the reactions happen, generally Low temperatures promote CO conversion thermodynamically, while pressure has little influence because the process is exothermic and

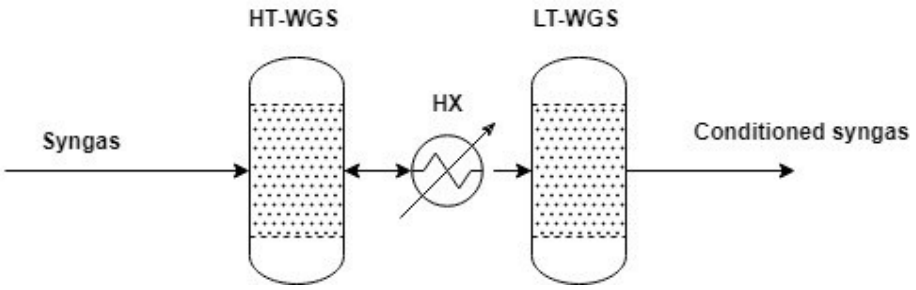

Figure 3.6 The WGS reactors

has no mole number variation [55].

For changing the thermodynamic equilibrium conversion and regulating the reaction rate in the water gas shift reactor, the H_2O/CO feed molar ratio generally varies from 2 to 5 [55]. To achieve the required H_2/CO ratio, a bypass syngas stream mechanism can be seen in Figure 3.7. The feed from the autothermal reformer is also mixed with the clean syngas from the syngas cleaning unit.

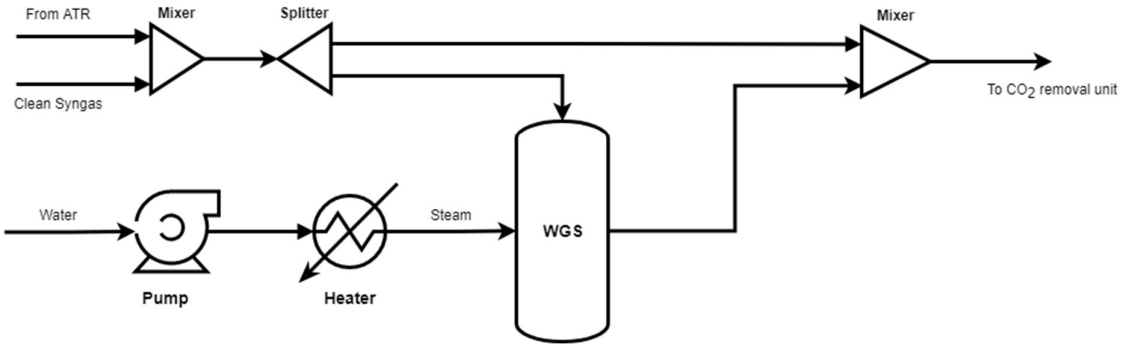

Figure 3.7 Syngas Conditioning Unit

3.6 Fischer-Tropsch process

The Fischer-Tropsch synthesis process is a prominent method to convert syngas to liquid fuel. The FT synthesis is a catalytic process that requires syngas mostly consisting of hydrogen (H_2) and carbon monoxide (CO) and produces a wide range of hydrocarbons. The operating mode, kind of catalyst employed, and reactor design are all important elements in the FTS sections. The syngas conversion efficiency, as well as the product distribution of the feeds for the product upgradation section, are determined by these process variables. The operational mode can be either High-Temperature Fischer-Tropsch (HTFT) or Low-temperature Fischer-Tropsch (LTFT).

The HTFT mode uses Fe-based catalysts at temperatures between 320 and 375^{o}C in the reactor. The HTFT is a dual-phase system (solid and gas). In this process, more gasoline and low hydrocarbon such as CH_4 will dominate the product of FT crude. The LTFT mode is typically between 200 and 240^{o}C, either using Fe or supported with Co-based catalysts. This mode produces paraffin and high molecular mass hydrocarbon such as waxes with great selectivity. The LTFT is a three-phase system with solid, liquid, and gas components.

Table 3.3 HTFT and LTFT comparison [42]

Property	HTFT	LTFT	Crude Oil
Paraffins	>10 %	Major product	Major product
Naphthenes	<1 %	<1 %	Major product
Olefins	Major product	>10 %	none
Aromatics	5-10 %	<1 %	Major product
Oxygenates	5-15 %	5-15 %	<1 % O(heavy)
Sulfur species	none	None	0.1-5 % S
Nitrogen Species	none	None	<1 % N
Water	Major by-product	Major by-product	0-2 %

The FT method produces a multicomponent combination of low to high carbon range hydrocarbon crude. The FT synthesis chemistry can be divided into three categories [56]:

- Major reactions: methane formation, formation of paraffin and olefins, WGS reactions

- Side reactions: alcohol formation and carbon deposition reactions
- Solid-phase reactions: carbides and oxides formation reactions

the general reactions are presented below:

- Methane: $$CO + 3H_2 \rightarrow CH_4 + H_2O \quad (10)$$
- Paraffins: $$(2n+1)H_2 + nCO \rightarrow C_nH_{2n+1} + nH_2O \quad (11)$$
- Olefines: $$(2n)H_2 + nCO \rightarrow C_nH_{2n} + nH_2 \quad (12)$$
- WGS reaction: $$CO + H_2O \rightarrow CO_2 + H_2 \quad (13)$$
- Alcohols: $$2nH_2 + nCO \rightarrow C_nH_{2n+1}OH + nH_2O \quad (14)$$
- Boudouard reaction: $$2CO \rightarrow C + CO_2 \quad (15)$$

- Catalyst oxidation/reduction: $$M_xO_y + yH_2 \rightarrow yH_2O + xM \quad (16)$$

$$M_xO_y + yCO \rightarrow yCO_2 + xM \quad (17)$$

- Carbide formation: $$yCO + xM \rightarrow M_xC_y + yC \quad (18)$$

$$yCO_2 + xM \rightarrow M_xC_y + yCO \quad (19)$$

As the Fischer-Tropsch process is a polymerization reaction, it produces a wide range of products with varying carbon chain lengths, such as the products mentioned above. Several reaction factors, such as temperature, pressure, catalyst type, and reactors, influence product selectivity. The distribution among these different carbon ranges can be explained by using Anderson-Schulz-Flory (ASF) definition. The result from the ASF model is an ideal distribution that predicts the final products of the FT process. According to ASF, the molar fraction (M_n) of the hydrocarbon product with a carbon number of n is simply reliant on the chain growth probability (α), which is a function of the rates of chain growth and chain termination [26], [56].

$$M_n = \alpha^{n-1}(1-\alpha) \quad (3.2)$$

the chain growth probability (α) is based on the experimental investigation and reported by Song as below [57]:

$$\alpha = \left(A * \frac{\gamma_{CO}}{(\gamma_{CO} + \gamma_{H2})} + B\right) * [1 - 0.0039(T - 533)] \quad (3.3)$$

where the T is the operating temperature in Kelvin and A and B are constants reported by [57] to be 0.2332 ± 0.0740 and 0.6330 ± 0.0420, respectively.

Iron and Cobalt are the dominant catalyst type used on the commercial scale. However, Nickel and Radium have higher selectivity in high carbon range hydrocarbons, but they need elevated pressure there is a possibility of the formation of volatile nickel carbonyl which is a drawback for the Ni catalyst. Ni selectivity of methane is also high at a higher temperature. Radium is the most active catalyst for FT synthesis, but it is also expensive and scarce[58]. The

cobalt-based catalyst works much better in FT synthesis with stoichiometric syngas due to its improved activity and selectivity for long-chain paraffin for use as synthetic diesel. A cobalt catalyst, however, is not suitable for sub-stoichiometric syngas feedstock because of its low WGS reaction activity. when Co is promoted by Ru, its reduction property increases, boosting its FT activity and selectivity for higher molecular weight hydrocarbons. Cobalt catalysts can yield a selectivity of more than 80% toward diesel fuel when paired with wax hydrocracking [59].

Cobalt catalysts cost more than iron catalysts. Thus, from an economic aspect, replacing the catalyst regularly is not feasible. Although supported cobalt catalysts offer high activity and selectivity to linear paraffin, as well as high resistance to deactivation, they perform poorly in the WGS process. Because the FT operating temperature for cobalt catalyst is low (220^{o}C), the formation of coke or free carbon which effect the catalyst performance is limited, whether through hydrocarbon breakdown or the Boudouard reaction [56].

It has been reported by Kim et al. [60] that CO2 acts as a moderate oxidizing agent on reduced Co/c-Al_2O_3 at 220 C and 20 bar. During the FTS process, CO2 addition reduces CO conversion and C_{5+} selectivity. The partial surface oxidation of cobalt metal caused by CO_2 exposure is responsible for the reduced catalytic activity and C_{5+} selectivity [60].

As previously stated, there are two types of FT processes: HTFT and LTFT, which are distinguished by their working temperatures. The reactors used in these processes have a long and rich history of invention, modification, and improvement. The FT-synthesis can be carried out in a fixed bed, slurry phase, or fluidized bed reactor, as stated by [25]. The fluidized bed reactors are designed for high-temperature FT processes and operate at temperatures ranging from 320 to 350 °C (HTFT), while the other two reactors operate at temperatures ranging from 220-to 250 °C (LTFT). The HTFT process is exclusively vapor-based, whereas the LTFT method may contain a liquid phase[23]. Figure 3.8 is presenting the schematic of these reactors.

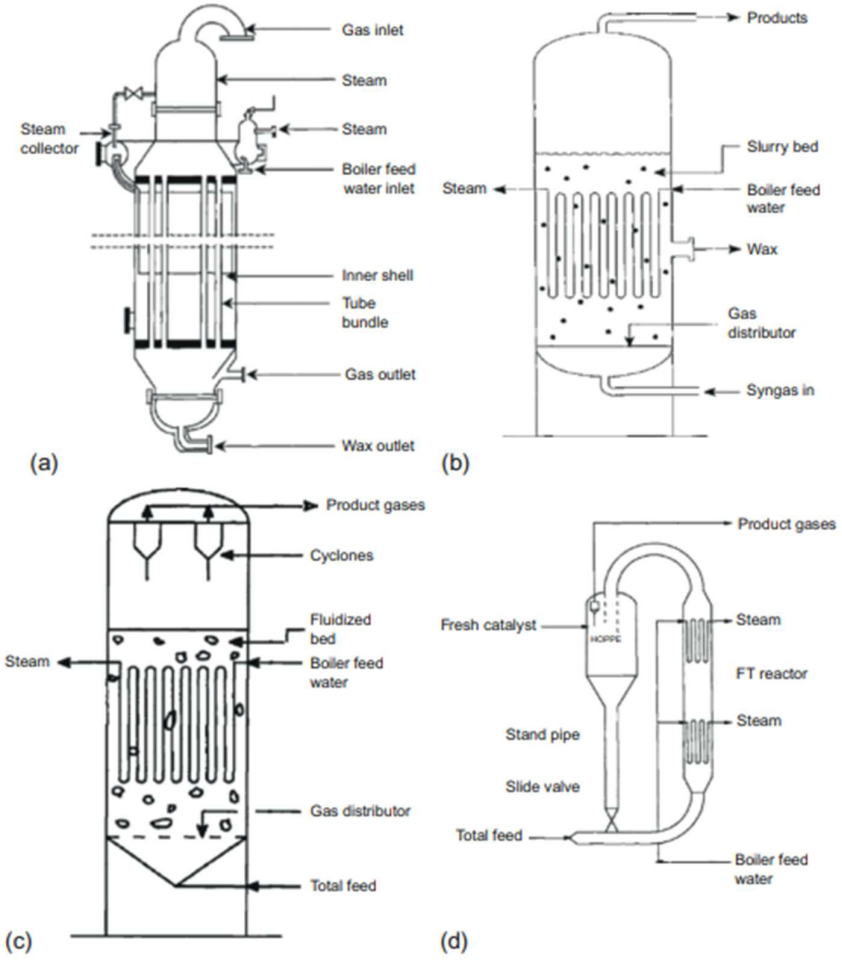

Figure 3.8 FT reactor types: (a) fixed bed reactor, (b) slurry phase reactor, (c) turbulent fluidized bed reactor and (d) Synthol circulating fluidized bed (CFB) reactor [56].

In the Fixed bed reactor type (Figure 3.8 a) the catalyst is often placed within tubes in these reactors, with the cooling medium positioned on the shell side. The use of tiny tubes leads to increased gas velocity and heat removal. These reactors often have a gas recycle option to improve percentage conversion. liquid hydrocarbon products can be recycled to improve the temperature profile in the bed. The catalyst particle size is generally small to ensure a large surface area for the reaction [56].

However, slurry phase reactors (Figure 3.8 b) have some advantages over tubular reactor types such as they are much less expensive reactors for the same capacity; the pressure drop over the reactor is greatly reduced; Because of the lower loading, the catalyst costs are less; more uniform temperature profile within the reactor, resulting in greater average temperature operation; catalyst removal and addition can be done online which allows for longer reactor runs and greater average conversion in this kind of reactor [56].

Depending on the velocity of the gas fluidized bed reactor (FB) can be either turbulent (Figure 3.8 b) or circulating mode (CFB) (Figure 3.8 C). Because of their increased heat transfer capabilities, FB reactors are suitable for the HTFT process. In the CFB mode, feed gas warmed

to 200°C sweeps the catalyst up the reaction section. The heat generated by the process is evacuated by tubular exchangers installed inside the reactor [56][15].

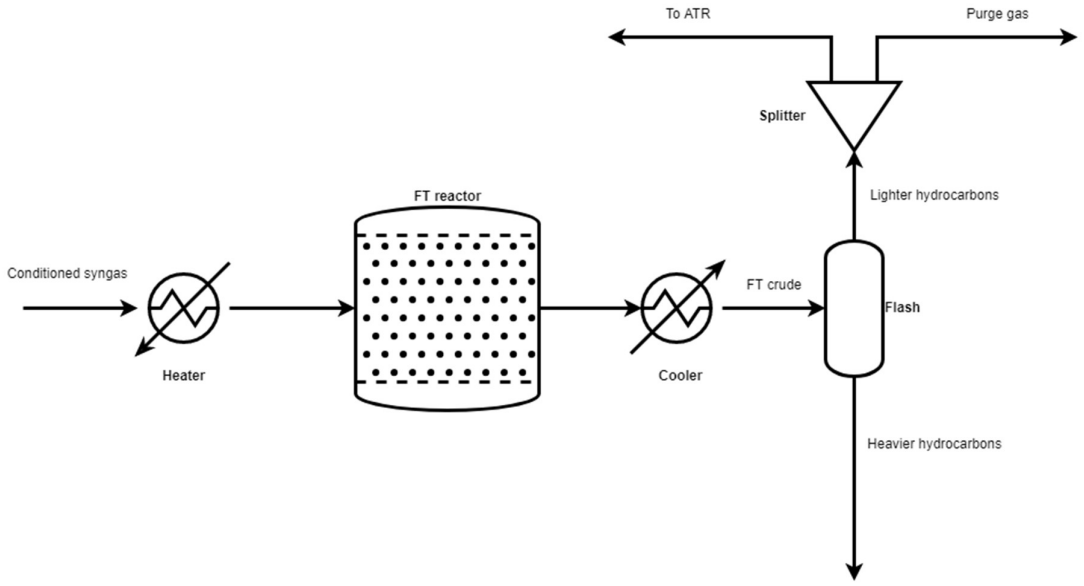

Figure 3.9 Fischer Tropsch Synthesis

Figure 3.9 shows the process after FT reactor. FT crude goes through a flash separator where lower hydrocarbons are separated from heavier hydrocarbons. The lower hydrocarbons are sent to an autothermal reformer with some fraction of gas being purged to avoid the accumulation of the inert nitrogen gas in the system.

3.7 Autothermal reformer

Autothermal reforming (ATR) uses oxygen and steam in a process with a low-carbon-range hydrocarbon to create synthesis (mainly CO and H_2). The reaction takes place in a single chamber where the hydrocarbon is partially oxidized. The reaction is exothermic due to oxidation. The capacity to alter H_2/CO is a significant benefit of autothermal reforming to produce certain biofuels. Figure 3.10 is illustrating the Autothermal reformer schematics.

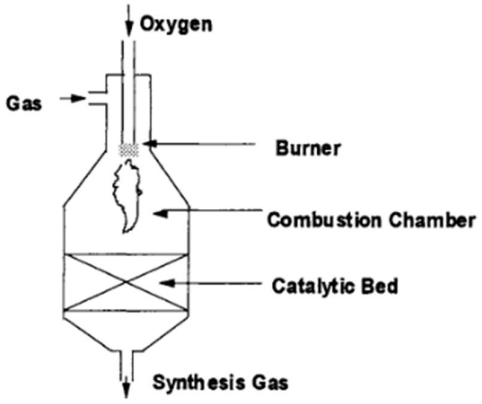

Figure 3.10 Autothermal reformer [61]

The autothermal reforming reactor consists of three zones:

- the burner in which feed streams get mixed
- the combustion zone, which produces a mixture of carbon monoxide and hydrogen
- the catalytic zone, where gases leaving the combustion zone achieve thermodynamic equilibrium.

The reaction occurs in a single chamber in which the hydrocarbon is partly oxidized. Because of the oxidation, the process is exothermic. ATR is a process that combines endothermic SR reactions with exothermic partial oxidation (POX) reactions (equations below).

$$CH_4 + \left(\frac{1}{2}\right) O_2 + \left(\frac{1}{2}\right) H_2O \rightarrow CO + \left(\frac{5}{2}\right) H_2 \quad (20)$$

$$CH_4 + \left(\frac{1}{2}\right) O_2 + \left(\frac{1}{2}\right) CO_2 \rightarrow \left(\frac{3}{2}\right) H_2 + \left(\frac{1}{2}\right) H_2O + \left(\frac{3}{2}\right) CO \quad (21)$$

$$C_nH_m + \left(\frac{m}{4}\right) O_2 + 2\left(n - \frac{m}{4}\right) H_2O \rightarrow nCO + 2nH_2 \quad (22)$$

$$C_nH_m + ((n-1)/2)\, O_2 + CO_2 \rightarrow (n+1)CO + \left(\frac{m}{2}\right) H_2 \quad (23)$$

The thermoneutrality of an autothermal reactor is governed by the values of n and m in the equations above. The first segment of the reactor should be filled with a Partial Oxidation catalyst, followed by a Steam Reformer (SR) catalyst in the second segment. In this technique, the heat generated by the exothermic POX reaction is carefully coupled with the heat requirement of the endothermic SR reaction [62].

According to the literature, there are several advantages of using an autothermal reformer in the process such as [62]:

- Compact design, resulting in a smaller related footprint.
- Inexpensive investment.
- Economy of scale.
- Flexible operation with quick starting durations and rapid load adjustments.
- Soot-free operating.

3.8 Techno-economic analysis

The economic feasibility of biofuels technologies must be determined before they can be considered as an alternative to fossil fuel-based processes for aviation fuel production in commercial applications. A feasibility analysis is sometimes known as techno-economic analysis because it combines the technological and economic components of a project. The fundamental theoretical configuration is first created, followed by a mass and energy balance which was explained in the previous sections. Second, the cost estimate allows for the calculation of biomass conversion technology and production costs for the BtL. Many techno-economic studies on power generation and biofuel scenarios have been conducted as interest in bio-renewable resources has grown due to the CO_2 tax and the EU 2050 vision for reduction of the energy sector be dependent on the fossil fuel. The accuracy of these investigations' results is generally around 30% of the total cost [63].

Research and development (R&D), engineering, and business are all connected via techno-economic modeling (TEM) or techno-economic analysis (TEA). Techno-economic analysis (TEA) is a method of evaluating the economic performance of a process by determining the most appropriate mix of technologies that would yield the greatest economic results. It can help organizations better understand the elements that impact the profitability of their technology development initiatives by correlating process parameters to financial parameters [64].

The process for cost evaluation starts with the raw material and process followed by the product prices. the raw material can be divided into different parts such as the market prices, logistics, and pretreatments. the process cost count for the capital, operation, and maintenance costs of the plant. The capital cost will be mainly the equipment cost which is found based on the literature and scaled based on the size. the operation cost will be the energy requirement and labor which can be broken down into personnel costs, maintenance & insurance, catalysts, chemicals, and oxygen carrier. The product prices will depend on the yield of fuel that is produced in the process and the selling prices which will be an estimate based on present market prices [65].

Previous studies on economic performances of producing jet fuel from cornstalk using Dual fluidized bed gasification and Low-temperature Fischer Tropsch technologies have been evaluated and reported the cost depending on the process between 124–141 €/MWh [46][66]. The FT diesel production cost based on the forest residue was reported as 125-130 €/MWh in the study done on techno-economic analysis and georeferenced for the HTFT process [50].

4 Methodology

This chapter explains the Aspen Plus model for simulating a BtL process for the production of bio-aviation fuel along with assumptions about the process conditions. Moreover, it also explains the steps for technoeconomic analysis, and the necessary assumptions involved with it.

4.1 Operating Conditions and Assumptions

Table 4.1 indicates the set of conditions and assumptions for a base case evaluation.

Table 4.1 Base case model conditions

Base Case Conditions	
Raw Biomass Moisture Content	50 %
Biomass Moisture Content After Drying	15 %
Gasification Steam Temperature	500 °C
Fuel Reactor Temperature	935 °C
WGS Reactor Temperature	350 °C
Optimum H_2/CO Ratio for FT Synthesis [23]	2.1
Fischer Tropsch Synthesis Temperature	220 °C
Auto-thermal Reformer Temperature	1000 °C
Auto-thermal Reformer Steam Temperature	250 °C
Configuration	62 % CO2 capture efficiency for Amine scrubber, Sweet WGS reactor, Rectisol unit after WGS reactor

The composition for the raw biomass fuel (forest residue) is given in table 3.1 and is assumed to have 50% moisture content as received after which it goes through a drying process to reduce its moisture content to 15%. The char conversion in the fuel reactor is assumed to be 99%, this assumption is justified when compared with experimental data in the literature for the high temperatures and steam-to-biomass ratios which is the case in this study. Condori et al. (2021) reported a char conversion of 98.7% in the fuel reactor for a temperature of 930℃ and a steam-to-biomass ratio of 0.62 [22]. Moreover, the system has been modeled with no pressure losses for simplification, however, capital costs of compressors needed to cover the pressure loss have been considered in the techno-economic analysis. The pinch analysis to calculate the heat available for district heating is implemented in Aspen Energy Analyzer.

4.1.1 Tar and Methane Formation

It is assumed that tar is only composed of Phenol, Toluene, and Bio-oil. The approximation of methane and tar formation is based on the experimental data found in the literature [21], [22]. The values for methane and tar formation at a fuel reactor temperature of 935℃ using different oxygen carriers are reported in Table 4.2.

Table 4.2 Methane and Tar formation assumptions

Methane and Tar formation at a fuel reactor temperature of 935 °C		
	LD Slag	Ilmenite
Methane	8 vol % of dry syngas	10 vol % of dry syngas
Tar	3 g/kg of dry biomass	1.5 g/kg of dry biomass

4.1.2 Oxygen Carrier

The model has been run for oxygen carriers such as LD-slag and Ilmenite as their experimental data for tar and CH_4 formation is available in the literature [21], [22]. LD slag is a by-product from the steel industry and is thus available at low cost and in significant quantities. Also, CaO in LD-slag acts as a catalyst for the water gas shift reaction resulting in a higher H2/CO ratio which is more favorable for the Fischer-Tropsch synthesis in this study [67]. Iron Titanium mineral, Ilmenite ($FeTiO_3$) is mined extensively and often used as oxygen carrier for chemical looping technologies [68]. The elemental compositions of LD-slag and Ilmenite are presented in Table 4.3.

Table 4.3 Oxygen carrier compositions

Composition (wt.%)	Fe_2TiO_5	Fe_2O_3	MnO_2	SiO_2	CaO	MgO	Al_2O_3	TiO_2	K_2O
LD-slag	-	26.6	3.3	11.9	39.8	9.1	1.2	1.3	<0.09
Ilmenite	54.7	11.2	-	5.5	-	-	-	28.6	-

In our model, pseudo brookite (Fe_2TiO_5) is defined as Fe_2O_3 +TiO_2, whereas ilmenite ($FeTiO_3$) is defined as FeO + TiO_2 where TiO_2 is an inert component [42].

4.2 ASPEN Plus Modelling

The property method chosen in the process model is the Peng-Robinson equation of state with Boston-Mathias modifications (PR-BM) and the stream class is set as MIXCINC which consists of three sub-streams: MIXED, Conventional Inert (CI) Solid, and Non-Conventional (NC) Solid. Sub-stream 'MIXED' consists of all the compounds in the vapor or liquid phase whereas the sub-streams 'CI Solid' and 'NC Solid' consist of all solid compounds with and without defined molecular weights, respectively. Biomass and ash are modeled as NC solids whereas char (graphite) and OC streams are set as CI solids. The enthalpy and density of biomass are calculated using 'HCOALGEN' and 'DCOALIGT' models in Aspen Plus respectively. Also, the heat of combustion on a dry basis is specified in Aspen Plus to calculate the enthalpy of biomass using the HCOALGEN model.

As per Figure 2.1, the biomass is first dried in a Biomass Drying Unit followed by a Chemical Looping Gasification (CLG) unit to produce syngas with some impurities. The syngas then goes through a series of equipment where solid particles, tars, hydrogen sulfide, carbon dioxide, ammonia, and nitrogen are removed. The clean Syngas is then conditioned using a Water Gas Shift (WGS) reactor to adjust the H_2/CO ratio to 2.1 before the Fischer Tropsch (FT) reactor. Syngas from the WGS reactor goes into a Rectisol unit to remove carbon dioxide and condensed water after which it enters the FT reactor. In the FT reactor, the syngas is

converted into hydrocarbons with carbon numbers ranging from 1 to 40 using the 'Anderson Schultz Flory' distribution. In the FT crude, heavier hydrocarbons are separated from the lighter hydrocarbons using a flash separator. The heavier hydrocarbons are sent to a refinery for upgradation into aviation fuel whereas the lighter hydrocarbons pass through a reformer before re-entering the FT reactor. In reformer, lighter hydrocarbons are converted back into Syngas using steam to improve the yield of heavier hydrocarbons in the FT crude. The FT crude is later distilled in CDU into different fuel fractions.

4.2.1 Biomass Drying

The biomass drying unit (Figure 4.1) is modeled using an RStoic reactor block **1** and a Separator block **2**. RStoich **1** is a stoichiometric reactor based on known fractional conversions or extents of reaction. In RStoic block **1**, the biomass is heated at a pressure of 1 bar to

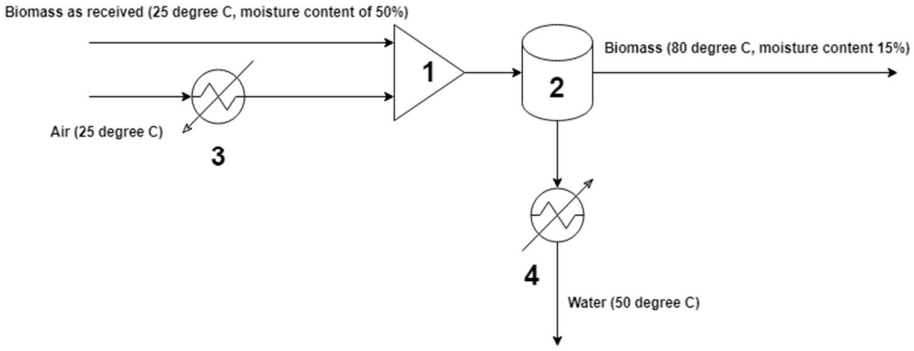

Figure 4.1 Biomass Drying Unit

evaporate the moisture content in the biomass using air that is heated to 200 degrees Celsius in a heater block **3**. The mass. There is a Design Spec block to adjust the air flowing into the RStoic block such that the biomass reaches a temperature of 80 degrees Celsius after drying. RStoic block is followed by a Separator block **2** to separate the water vapors from the dry biomass after which the dry biomass enters the CLG unit for gasification. A calculator block used to control the extent of drying is adjusted to bring the moisture content in the biomass from 50 % down to 15 %. The air mixed with moisture is cooled down to 50 degrees Celsius using a cooler **4** to extract heat from the outgoing stream.

Table 4.4 Aspen Plus Model Description: Biomass Drying

Block	Aspen Model	Description	Unit
1	RStoic	Reaction: Biomass → 0.0555084 H_2O Since Biomass is an NC solid substream in Aspen plus, the software assumes the molar mass to be 1 g/mol. For only this reaction, the component attribute of biomass is changed such that it is 100% moisture. To reach the desired moisture level in the biomass, the fractional conversion for the above reaction is calculated by a calculator block using the following expression: $\frac{Moisture\ in\ wet\ biomass - Desired\ biomass\ moisture}{100 - Desired\ biomass\ moisture}$ Moreover, the block is also assumed to be adiabatic.	Belt Dryer
2	Sep	The component separator block completely separates the air and moisture from dry biomass.	
3	Heater	The outlet temperature is set to 200 degrees Celsius to heat the air needed for drying biomass.	Air Heater
4	Heater	The outlet temperature is set to 50 degrees Celsius to extract heat from the stream.	Cooler

4.2.2 Chemical Looping Gasification (CLG)

The CLG unit consists of a Fuel Reactor (FR) and an Air Reactor (AR) where metal oxide particles called Oxygen Carrier (OC) are reduced and oxidized, respectively. The oxygen carrier reduced in the FR enters the AR where it is oxidized again. This oxidized oxygen carrier then re-enters the Fuel reactor where it reacts with the biomass volatiles and reduces again, thus completing a loop. Moreover, it is assumed that no pressure losses occur in the CLG unit.

The CLG model (Figure 4.2) is adapted from Roshan et al. (2019) [69] with following modifications:

- Char leakage from FR to AR.
- Temperature control of FR/AR by controlling the circulation rate of OC.
- Closing the OC circulation loop.
- Modifications in reactor blocks.
- Controlling the methane and tar concentrations according to [21], [22]

In the Aspen Plus model, the gasifier is designed for a load of around 80 MW_{th} based on the LHV of the biomass entering the gasifier. The dry biomass from the biomass drying unit enters the FR where volatiles in the biomass reacts with the Fe_2O_3 in the OC and reduces it to Fe_3O_4

to provide sufficient energy for char gasification with steam which is a highly endothermic reaction as well as the devolatilization of biomass. Fe_2O_3/Fe_3O_4 is assumed to be the only redox pair for the transport of oxygen from AR to FR. The Fuel reactor is modeled using an RYield reactor block **1**, an RStoich reactor block **2**, and an RGibbs reactor block **3** to simulate the devolatilization of biomass (pyrolysis), char gasification (reduction), and combustion of volatiles. RYield **1** is a nonstoichiometric reactor based on known yield distribution whereas RGibbs **3** is a chemical equilibrium reactor that uses Gibbs free energy minimization to calculate equilibrium.

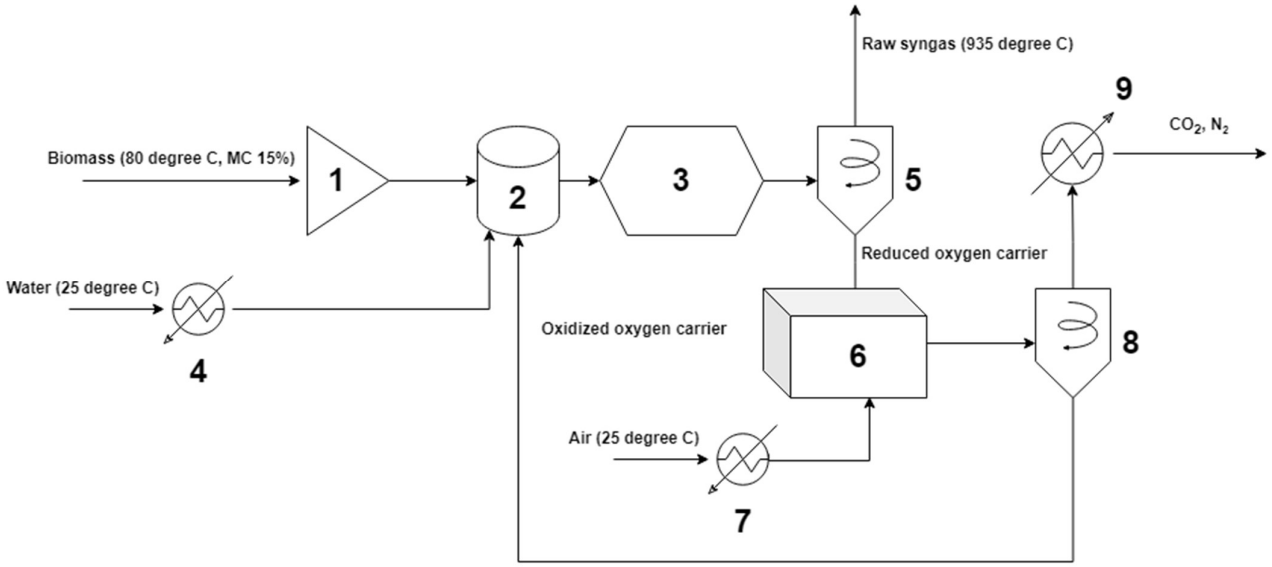

Figure 4.2 Chemical looping gasification

The RYield reactor **1** uses a calculator block to calculate the mass of constituent elements in the biomass, based on its proximate and ultimate analysis and converts biomass into the molecular forms of the constituent elements. The heat required in the RYield reactor **1** is provided by the combustion of volatiles in the RGibbs reactor **3**.

RStoich block **2** is modeled as an adiabatic reactor where primarily char gasification occurs with steam as a gasification agent. Steam is supplied to the RStoic reactor **2** at a pressure of 1 bar and a temperature of 500 degrees Celsius using a heater **4** with a steam to biomass ratio of 0.7 where it reacts with char to form carbon dioxide along with carbon monoxide and hydrogen (syngas). Apart from char gasification, conversion of biomass sulfur and nitrogen into hydrogen sulfide and ammonia respectively as well as methane and tar formation in the fuel reactor are also modeled in the RStoich block **2**. It is assumed that all sulfur converts into hydrogen sulfide whereas 60 percent of nitrogen converts to ammonia and the remaining 40 percent converts to nitrogen gas. Moreover, calculator blocks are used to achieve desired methane and tar compositions in the syngas stream exiting the FR based on experimental results in the literature by calculating the fractional conversion of carbon for methane and tar formation reactions in the RStoic reactor **2** and then feeding it back to the RStoic reactor **2**. Only 1% of the char is assumed to be unconverted which is implemented using a design spec that adjusts the extent of char gasification in the RStoic reactor **2**. The assumption is in line with the experimental data in the literature for the gasification of biomass at high

temperatures and steam to biomass ratios [22]. All the unconverted char in the FR leaks to the AR where it gets combusted with air into carbon dioxide and leaves with flue gases.

The gases from the RStoic reactor **2** enter the RGibbs reactor **3** where they react with Fe_2O_3 in the OC and reach a chemical equilibrium based on the minimization of Gibbs free energy. All Fe_2O_3 in the OC is reduced to Fe_3O_4 as some of the gases are combusted to provide energy for the RYield reactor **1** and to reach the desired temperature in the RGibbs reactor **3**. Char, methane, and tars are set as inerts in the RGibbs reactor **3** to control their concentration in the syngas stream exiting the FR. A design spec that is used to control the temperature of the RGibbs reactor **3** by changing the circulation rate of OC is set to operate the FR at 935 degrees Celsius. Hence, the syngas and the reduced OC coming out of the FR have a temperature of 935 degrees Celsius. An SSplit block **5** is used to model a cyclone separator that separates OC from syngas. Syngas goes to the 'Syngas Cleaning Unit' whereas OC goes to the AR.

Air Reactor is modeled using an adiabatic RStoich block **6** where the leaked char is completely combusted, and all Fe_3O_4 in OC is oxidized back to Fe_2O_3 using a calculator block that provides the stoichiometric amount of air to the block. The air entering the AR is preheated to 450 degrees Celsius using a heater block **7**. Depleted air and carbon dioxide from char combustion are separated from the OC using an SSplit block **8**. Carbon dioxide is released into the air whereas the oxidized OC circulates back to the FR.

Table 4.5 Aspen Plus Model Description: Chemical Looping Gasification

Block	Aspen Model	Description	Unit
1	RYield	A calculator block is used to calculate the mass yields of all the components according to the component attribute of the biomass. There is a heat stream from RGibbs reactor **3** to provide heat for the decomposition of biomass.	Fuel Reactor
2	RStoic	Calculator blocks are used to control fractional conversion for the char gasification, tar formation, and methane formation reactions in the RStoic block to get the syngas composition according to the experimental studies. The fractional compositions for conversion of biomass nitrogen into ammonia and sulfur into hydrogen sulfide were specified according to assumptions. A calculator is used to control the flow of steam for the desired steam to biomass ratio. The block is adiabatic with no pressure loss.	
3	RGibbs	The products in this block are specified as per experimental data in [21], [22]. Biomass char, tar, methane, ammonia, and hydrogen sulfide are specified as inerts in the RGibbs reactor to achieve the desired tar, methane, ammonia, and hydrogen sulfide compositions in the syngas. A design spec block is used to adjust the circulation rate of oxygen carriers to provide heat to the decomposition of biomass in the RYield block as well as maintain the temperature of the RGibbs block at 935 degrees Celsius.	
4	Heater	Water is superheated to 500 degrees Celsius under atmospheric conditions.	Steam Boiler
5	SSplit	Syngas and fly ash are separated from the oxygen carrier. It is assumed that all the ash gets converted into fly ash.	Cyclone Separator
6	RStoic	Char that leaks with the oxygen carrier is combusted along with the oxidation of the reduced oxygen carrier with a stoichiometric amount of air provided to the block with the help of a calculator block.	Air Reactor
7	Heater	Air supplied to the Air Reactor is preheated to 450 degrees Celsius.	Air Heater
8	SSplit	Flue gas/depleted air is separated from the oxidized oxygen carrier.	Cyclone Separator
9	Heater	Flue gas/depleted air-cooled to 50 degrees Celsius to recover heat from the hot stream.	Flue gas Cooler

4.2.3 Syngas Cleaning

The Syngas cleaning model (Figure 4.3) is adapted from the gas cleaning model developed by Arvidsson et al. (2014) [70], however, the pressure losses have been assumed to be zero. Syngas from the CLG unit contains ash, tar, water, nitrogen, carbon dioxide, and hydrogen sulfide as impurities that need to be removed. In this study, the temperature out of the fuel reactor is 935 degrees Celsius which is not in the range of working temperature for ESPs. Therefore, cold syngas cleaning is required for the impurity removals. The syngas before EPS is cooled down based on studies by Arvidsson et al. [70]. It is assumed that all the ash in biomass is fly ash which is completely removed from syngas using a particulate separator modeled as an SSplit block **2** after cooling the syngas down to 210 degrees Celsius using a cooler **1**.

The syngas then goes into a cooler **3** where syngas is cooled to 110 degrees Celsius before entering the Rapeseed Methyl Ester (RME) Scrubber where a stream of RME mixes with syngas absorbing all the tar components in the syngas. The RME scrubber is modeled as a combination of component separator (Sep block) **4** and flash separator (Flash2 block) **5** in Aspen Plus. The mass flow of RME is controlled using a design spec such that the RME consumption, on an HHV basis, is 2.4 % of the syngas stream leaving the scrubber [70]. Ash and tar-free syngas go through a flash separator (Flash2 block) **5** where most of the water content and some ammonia is removed.

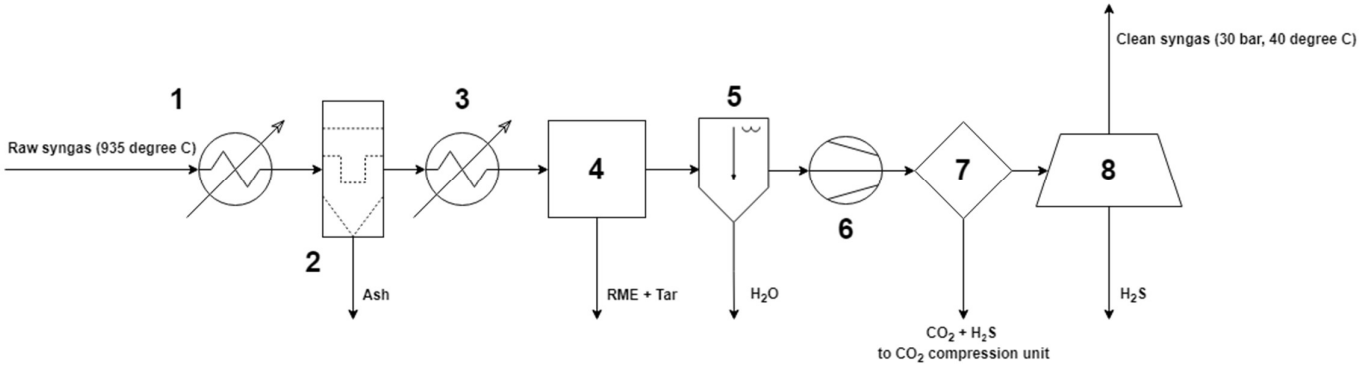

Figure 4.3: Syngas Cleaning Unit

The syngas is then compressed using a 3-stage compressor **6** (with intercoolers and knockout drums) to a pressure of 30 bar before passing through a conventional Amine Absorber **7** and later through a Zinc-oxide Guard bed **8** where the remaining unwanted gases are removed. Both amine absorber **7** and guard bed **8** are modeled as Sep (component separator) blocks and require 3.3 MJ of energy for every kilogram of CO2 and H_2S captured. The amine absorber **7** uses methyl diethanolamine (MDEA) solvent with H_2S, CO2, NH_3, CH_4, and CO molar capture efficiencies of 96 %, 62 %, 100 %, 0.0738 %, and 0.0581 % respectively whereas the zinc-oxide guard bed **8** removes any traces of H_2S remaining in the syngas before syngas goes to a water gas shift reactor for conditioning, where even small traces of H_2S can poison the catalyst for a sweet WGS reactor. There is no loss of pressure assumed in any of the equipment in the gas cleaning process, so the clean syngas exits the syngas cleaning unit with a temperature of 40 degrees Celsius and a pressure of 30 bar.

Table 4.6 Aspen Plus Model Description: Syngas Cleaning

Block	Aspen Model	Description	Unit
1	Heater	The raw syngas from the fuel reactor is cooled down to 210 degrees Celsius.	Cooler
2	SSplit	The fly ash is separated from the syngas stream.	Fabric Filter
3	Heater	The syngas is ash-free syngas is further cooled down to 110 degrees Celsius	Cooler
4	Sep	Syngas stream from the syngas cooler and RME stream at 25 degrees Celsius go into the block where RME and tar components are removed from the syngas by the component separator block to simulate an RME absorber with RME acting as a scrubbing liquid. A calculator block is used to control the flow of RME into the block such that the energy content of RME is 2.4 % of the outlet syngas on an HHV basis.	RME Absorber
5	Flash2	Water is also removed from the syngas in the RME absorber which is simulated by this block.	
6	MCompr	Ash and tar-free syngas are compressed to a pressure of 30 bar using an isentropic 3-stage compressor with equal pressure ratios across all the stages. The coolers after the first and second stages have an outlet temperature of 40 degrees Celsius whereas the cooler after the third stage has an outlet temperature of 80 degrees Celsius. There are also knockout drums between the stages which remove liquid components from the syngas stream.	Syngas Compressor
7	Sep	96 %, 62 %, 100 %, 0.0738 %, and 0.0581 % (on a molar basis) of H_2S, CO_2, NH_3, CH_4, and CO respectively are removed from the syngas stream by the component separator block to simulate an amine absorber	Amine Absorber
8	Sep	100 % H_2S is removed from the syngas stream.	Zinc Oxide Guard Bed

4.2.4 Syngas Conditioning

The Syngas conditioning model (Figure 4.4) is also adapted from the model developed by Arvidsson et al. (2014) [70], however, the pressure losses have been neglected. Syngas from the cleaning unit mixes with the syngas from ATR using a mixer block **4** before entering a stream splitter (FSplit block) **5** which is controlled by a design spec to reach the desired H_2/CO ratio (preferably 2.1 for Co catalysts) before the FT reactor [23]. The stream splitter **5** splits the stream into two, one of which bypasses the Water Gas Shift (WGS) reactor **3** whereas the other goes to a heater block **6** where the syngas is heated up to 350 degrees Celsius before entering the WGS reactor **3**, modeled as an adiabatic RGibbs block, where water gas shift

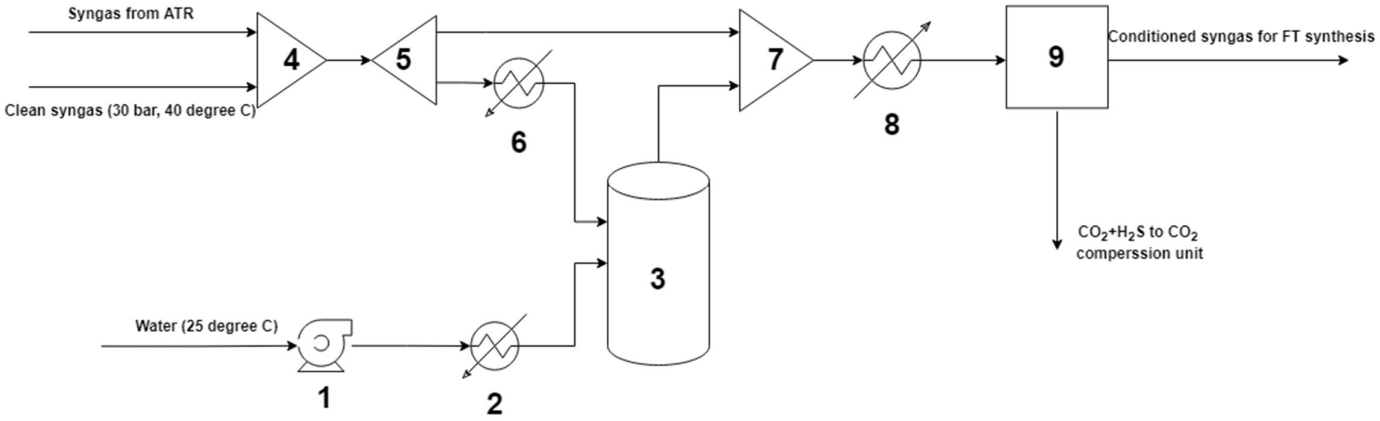

Figure 4.4: Syngas Conditioning using Water Gas Shift Reactor

reaction occurs between steam and syngas at 350 degrees Celsius and 30 bar pressure resulting in the formation of more H_2 and CO_2.

The water is pumped to 30 bar pressure using a pump block **1** and then superheated to 350 degrees Celsius using a heater block **2** before entering the WGS reactor block **3**. The stream exiting the WGS reactor mixes with the bypass stream using a mixer block **7** before going through a Rectisol unit, modeled as a heat exchanger block **8** that cools down the syngas to -12 degrees Celsius, and a Sep2 block **9**, where all the H_2O and 96.8 % moles of CO_2 are removed from the syngas.

Table 4.7 Aspen Plus Model Description: Syngas Conditioning

Block	Aspen Model	Description	Unit
1	Pump	Water is pumped to a pressure of 30 bar with a pump efficiency of 90 %.	Water Pump
2	Heater	Water is superheater to a temperature of 350 degrees Celsius.	Steam Generator
3	RGibbs	The block is an adiabatic RGibbs reactor. The products of the WGS reaction expected in this block are specified by the user. Methane is specified as inert in the RGibbs reactor. There is a design spec block to control the flow of steam such that the H_2O/CO ratio in the reactor block is 3:1 to avoid carbon deposition in the reactor.	WGS Reactor
4	Mixer	Syngas stream from ATR and syngas stream from the Syngas Cleaning Unit are mixed in this block.	Mixer
5	FSplit	This block splits the syngas stream after the mixer into two, one of which goes to the WGS reactor and the other bypasses the WGS reactor. The splitting ratio is adjusted by a design spec block to achieve an H_2/CO ratio of 2.1 before the FT reactor.	Splitter
6	Heater	The syngas is heated to 350 degrees Celsius before entering the WGS reactor.	Heater
7	Mixer	The syngas from the WGS reactor and the bypass syngas are mixed in this block	Mixer
8	Heater	The syngas is cooled down to -12 degrees Celsius which simulates the refrigeration of syngas in the Rectisol unit.	Rectisol
9	Sep2	All the water and 96.8 % moles of CO_2 are removed from the syngas stream. A calculator block controls the amount of steam needed for regeneration of the scrubbing liquid in the Rectisol such that 6.97 kg of 5 bar steam is supplied for every kmol of CO_2 and H_2S captured. Other than refrigeration, 1900 kJ of electricity is needed for each kmol of CO_2 or H_2S captured whereas the electricity needed for refrigeration is 3 times the duty of block 8 [36], [65].	

4.2.5 Fischer Tropsch (FT) Synthesis

The FT synthesis model (Figure 4.5) has been adopted from Pondini et al. (2013) [71]. The syngas from the Rectisol unit is heated to 220 degrees Celsius in heater **1** before entering the FT reactor **2** which is modeled as an RStoich reactor with a 70 % CO conversion corresponding to the selection of Cobalt as the catalyst. Higher CO conversion requires the use of advanced

catalysts in large amounts, however, CO conversion of even up to 90 % has been assumed in some studies, so a moderate assumption of 70 % is justified [72]. The fractional conversions of the reactions in the FT reactor are controlled by a calculator to form hydrocarbons with carbon numbers ranging from 1 to 4 according to the carbon selectivities given by Rane et al. (2012) using cobalt catalyst and hydrocarbons with carbon numbers ranging from 5 to 40 using the 'Anderson Schultz Flory' distribution [73].

The hydrocarbons from the FT reactor are cooled down to 30 degrees Celsius in a cooler **3** before going through a Flash2 separator **4** which removes most of the water content from the FT crude and separates lighter hydrocarbon vapors (mainly consisting of hydrocarbons with carbon numbers ranging from 1 to 4) from the heavier hydrocarbons in the liquid state. Since we aim to increase the yield of aviation fuel, hydrocarbons with carbon numbers ranging from 8 to 16 are desired [74]. For this reason, the lighter hydrocarbons are recycled back to the WGS reactor for conditioning after passing through an autothermal steam reformer **6** modeled as an adiabatic RGibbs reactor where they react with steam and convert back to syngas. The steam is provided by pumping water to 30 bars using a pump block **7** and then superheating it to 250 degrees Celsius with a heater block **8**. A small amount of O_2 is also introduced into the reactor to combust with the hydrocarbons and reach the desired reforming temperature of 1000 degrees Celsius. The water formed because of steam reforming is removed using a flash separator (Flash2 block) **10** downstream.

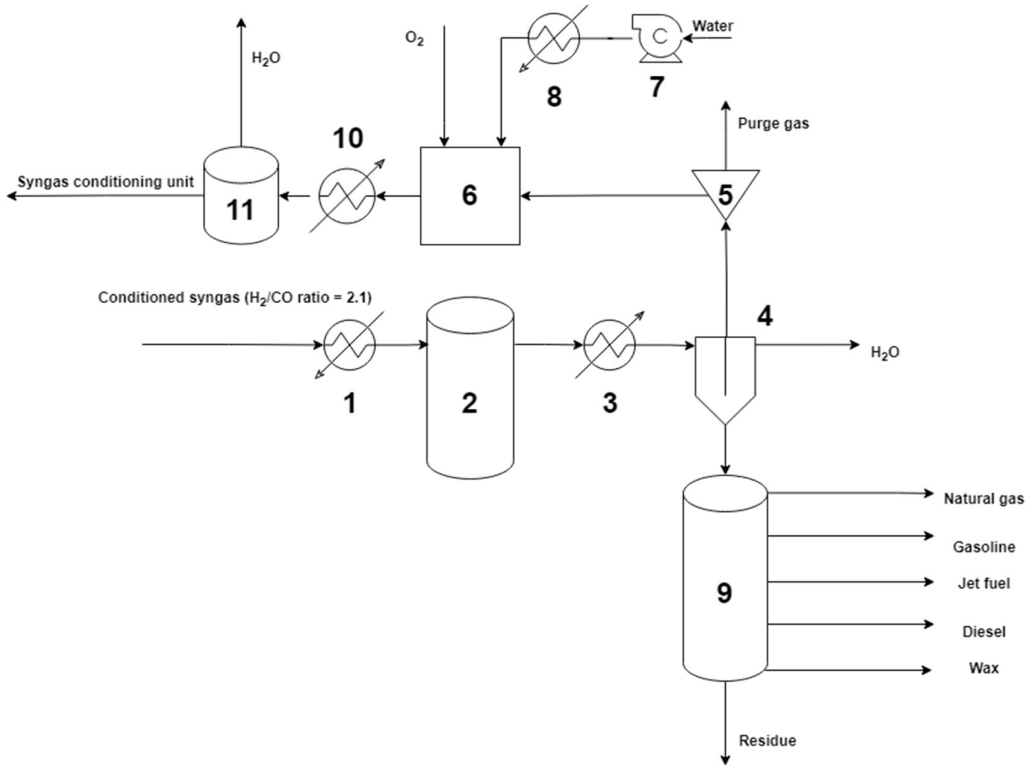

Figure 4.5: Fischer Tropsch Synthesis with Autothermal Reformer and Distillation of FT Crude

The FT crude from the flash separator **4** goes to a distillation column **9** where fuel fractions such as lighter hydrocarbon gas, gasoline, kerosene (jet A fuel), diesel, and wax with carbon numbers ranging from 1 to 3, 4 to 7, 8 to 16, 17 to 22, and 22+ respectively are separated.

The distillation column is modeled using a Sep block. The energy demand for distillation is fulfilled by consuming 2 percent of the FT crude [75].

Table 4.8 Aspen Plus Model Description: FT synthesis

Block	Aspen Model	Description	Unit
1	Heater	Syngas after the Rectisol unit is heated to 220 degrees Celsius for FT synthesis.	Syngas Heater
2	RStoic	The block operates at 220 degrees Celsius. A calculator is used to calculate the fractional conversion of CO for all the reactions mentioned in the block for the formation of Olefins and Paraffins with carbon numbers 1 to 40 from the syngas according to Anderson Schultz Flory distribution. The overall CO conversion in a single pass is set to be 70 %.	FT Reactor
3	Heater	The FT products from FT synthesis are cooled down to 30 degrees Celsius.	Cooler
4	Flash2	Water in the FT products is flashed out from the stream. Hydrocarbons with lower carbons (gaseous phase) are recycled back whereas hydrocarbons with longer chains (liquid phase) are sent to the distillation column.	Flash Separator
5	FSplit	The splitter splits the recycle stream to purge some gas to avoid the accumulation of inert gases such as nitrogen. 4 % of the recycle stream is purged off.	Purge Gas Separator
6	RGibbs	The block is an adiabatic RGibbs reactor. The products are specified as H_2O, CO, H_2, CO_2, and N_2. There is a design spec block to control the flow of O_2 such that the temperature of the block is maintained at 1000 degrees Celsius. The flow of steam into the ATR is controlled by a calculator block such that there is one mole of H_2O for each mole of carbon in the recycled FT stream.	Auto-thermal Reformer
7	Pump	Water is pumped to a pressure of 30 bar.	Water Pump
8	Heater	Water is superheated to a temperature of 250 degrees Celsius.	Steam Generator
9	Sep	FT crude is distilled into different liquid fractions. 2 % of FT crude is consumed for the energy requirements of the distillation column [75].	Distillation Column
10	Heater	The syngas from ATR is cooled down to 40 degrees Celsius.	Syngas Cooler
11	Flash2	Water and other liquid fractions are flashed out from the syngas.	Flash Separator

4.2.6 CO_2 Compression and Liquefaction

As seen in Figure 4.6 acid gases from Acid Gas Capture units go through a flash separator **1** to remove the moisture content before being compressed to 120 bars in a 3-stage CO_2 compressor **2** with equal pressure ratios across all the stages isentropically as per literature

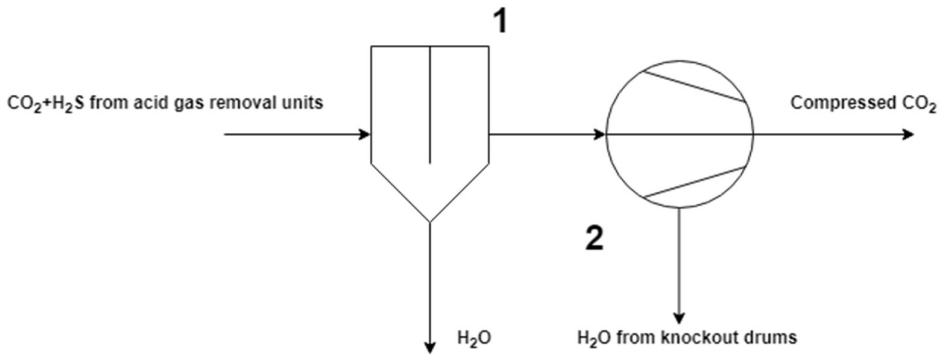

Figure 4.6: Carbon Dioxide Capture Unit

[76], [77]. There are also intercoolers and knockout drums between compressor stages to remove moisture from the acid gas stream. The outlet temperature for all the intercoolers is 40 °C.

Table 4.9 Aspen Plus Model Description: CO2 Compression

Block	Aspen Model	Description	Unit
1	Flash2	Syngas after the Rectisol unit is heated to 220 degrees Celsius for FT synthesis.	Flash Separator
2	MCompr	Residue streams from acid gas removal units are compressed to a pressure of 120 bar using an isentropic 3-stage compressor with equal pressure ratios across all the stages. The outlet temperature for all the intercoolers is 40 degrees Celsius. There are also knockout drums between the stages which remove liquid components from the stream.	CO_2 Compressor

4.3 Process Configurations

Carbon capture and storage (CCS) is a method for reducing manmade CO2 emissions. Physical and chemical absorption is regarded as the most close-to-market alternatives to be implemented at an industrial scale. However, these technologies are energy and operational cost-intensive for the biomass to liquid (BtL) processes as the cost will suppress the technology penetration in the market. Therefore, the process and technoeconomic effects of the removal of an AGR unit before the syngas conditioning unit have been investigated in this thesis. This means that the WGS reactor type changes from sweet to sour as syngas now contains sulphur contents as well. The different process configurations are given in Table 4.10.

Table 4.10 Different case configurations

Case	Configuration	WGS reactor catalyst type	Carbon capture efficiency
A	With Rectisol and Amine absorber	Sweet WGS	Amine absorber 62% Rectisol 97%
B	With Rectisol	Sour WGS	Rectisol 97%
C	With Amine absorber	Sour WGS	Amine absorber 62%
D		Sour WGS	Amine absorber 76%
E		Sour WGS	Amine absorber 90%

For the process configurations explained in Table 4.10, different carbon capture technologies with different carbon capture efficiencies are employed. All the other process parameters and units in the BtL plant remain exactly the same. Case A in Table 4.10 refers to the base case explained in Section 4.2 whereas cases B to E refers to the modified configurations with sour WGS reactors. Figures 4.7 and 4.8 illustrate the process configurations for sweet and sour WGS reactors respectively.

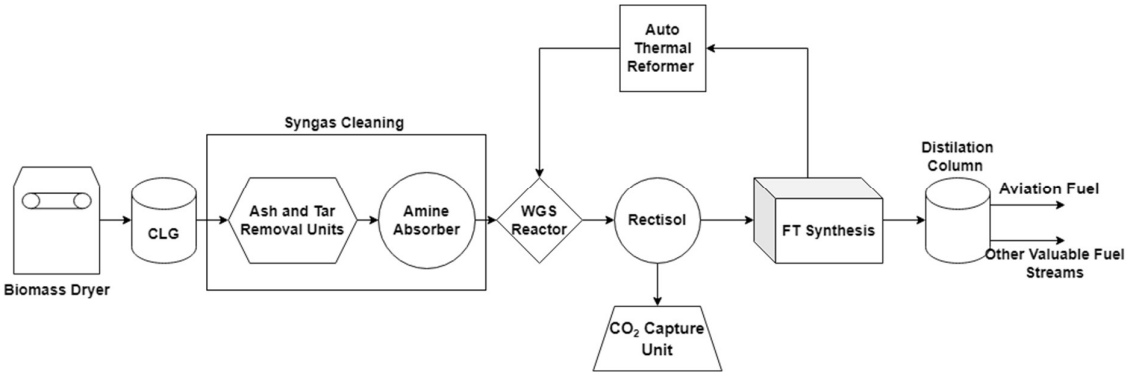

Figure 4.7 BtL configuration with sweet WGS reactor (Case A)

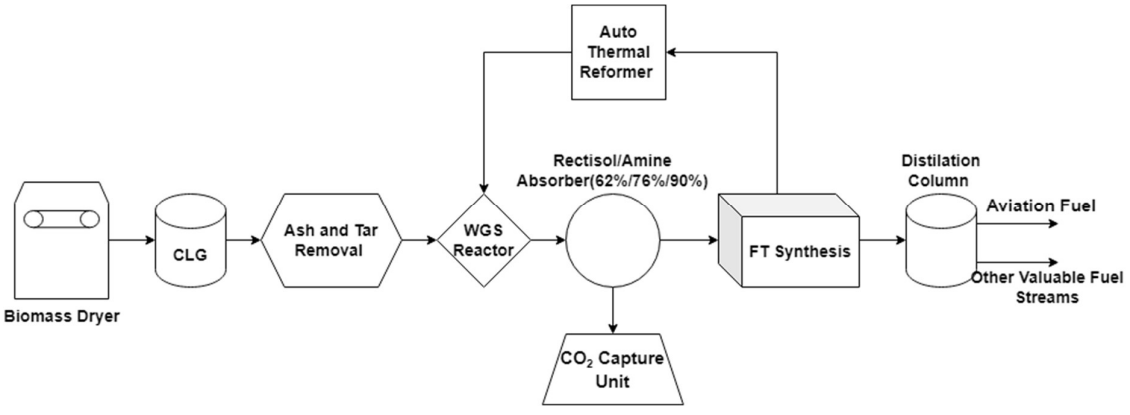

Figure 4.8 BtL configuration with sour WGS reactor (Cases B to E)

4.4 Process Parameters

In this section, some process parameters have been discussed for the evaluation of results and validation of the model with the experimental data.

4.4.1 Steam to Biomass ratio

The steam to biomass ratio is defined as the ratio of mass of steam entering the gasifier to the mass of biomass (including moisture) entering the gasifier.

$$\mathrm{S/B} = \frac{Steam\ entering\ the\ gasifier\ (kg)}{Biomass\ entering\ the\ gasifier\ including\ moisture\ (kg)} \quad (4.1)$$

4.4.2 Oxygen to Biomass ratio

The oxygen to biomass ratio λ is a molar ratio of oxygen consumed in the Air Reactor (AR) and the oxygen required for the stoichiometric combustion of biomass.

$$\lambda = \frac{2 * (O_{2,in} - O_{2,out})}{F_b * \Omega_b} \quad (4.2)$$

where $O_{2,\ in}$ and $O_{2,\ out}$ are the molar flow rates of oxygen gas entering and leaving the Air Reactor (AR) respectively, F_b is the mass flow rate of biomass entering the gasifier and Ω_b is the number of moles of oxygen required for stoichiometric combustion of biomass. The expression for calculating the number of moles of oxygen required for complete combustion of biomass is given as:

$$\Omega_b = x_C * \frac{2}{12} + x_H * \frac{1}{2} + x_S * \frac{2}{32} - x_O \quad (4.3)$$

where x_C, x_H, $x_{S,}$ and x_O are the mass fraction of carbon, hydrogen, sulfur, and oxygen in the biomass respectively.

4.4.3 Cold Gas Efficiency

The efficiency of the gasification process (including syngas cleaning) can be defined based on the cold gas efficiency which can be expressed as [10]:

$$CGE = \frac{mass\ flowrate\ of\ clean\ syngas * LHV\ of\ clean\ syngas}{mass\ flowrate\ of\ biomass\ (as\ received) * LHV\ of\ biomass\ (as\ received)} \quad (4.4)$$

4.4.4 Conversion Efficiency

The overall BtL (as received biomass to FT crude) process efficiency can be defined based on Conversion Efficiency (CE) given as:

$$CE = \frac{mass\ flowrate\ of\ FT\ crude * HHV\ of\ FT\ crude}{mass\ flowrate\ of\ biomass\ (as\ received) * HHV\ of\ biomass\ (as\ received)} \quad (4.5)$$

4.5 Techno-economic Analysis

This section contains information on the assumptions and data used in the techno-economic analysis of the study cases discussed in the methodology. The objective is to outline standard cost measures for evaluating the capital cost, operation cost, revenues, and financial measurements, as well as to detail relevant formulas. Table 4.11 highlights the underlying assumptions in our techno-economic analysis for the base case:

Table 4.11 Assumptions for the techno-economic analysis

Economic Lifetime of Plant (yrs)	20
Discount Rate (%)	10
Annual O&M Cost (%)	5
Annual Operating Hours (hrs/yr)	8000
Biomass Residue Chips Price (Euros/GJ)	5
Electricity Price (Euros/GJ)	14
District Heating Price (Euros/GJ)	1

The capital cost for smaller equipment such as compressors for pressure loss makeup, pumps, and heat exchangers is assumed to be 10% of the Total Plant Investment (TPI). The operation and maintenance cost of the case studies is assumed based on studies reported by Hannula et al.[65]. The O&M cost breaks down to personnel costs, maintenance and insurance, catalysts, and chemicals. In the base case studies, it was assumed to be 5% of the total plant cost while in the cases with sour water gas shift reactors, when studying the different process configurations, due to higher cost of the catalyst in the WGS reactor, 1 % was added to the O&M costs. The biomass residue and the electricity cost were estimated based on the studies done by [36], [66], [78] which use the same cost for their cost estimation. As the location of the plant is not considered in the thesis the value for selling the heat is considered negligible at 1 Euro per/ GJ.

4.5.1 Expenditure

The total annual cost includes the annual capital cost which is usually returned to the bank as a yearly installment of the loan taken from the bank for the construction of the plant and annual O&M cost which is usually taken as 5 % of the Total Plant Cost (TPC), annual fuel cost and annual electricity cost.

4.5.1.1 Capital Cost

The capital cost for the process includes the capital costs for civil works, feedstock handling, biomass belt dryer, atmospheric indirect gasifier, fabric filter, RME scrubber, amine scrubber, zinc guard bed, syngas compressor, CO2 compressor, WGS reactor, FT reactor (with HX), ATR and HC recovery (distillation). The cost of the equipment was estimated based on the literature.

The following procedure has been adopted for estimating the capital costs of a greenfield plant based on the data from the Aspen Plus model:

The data for capital costs of equipment was used to scale it up or down according to the size requirements based on the model calculations using the following equation:

$$C = C_0 * (\frac{S}{S_0})^f \quad (4.6)$$

where C_o (reference cost) is the cost for the equipment in literature for size S_o and C is the cost of the same equipment for the size S suggested by the model.

The scaling factor f usually range between 0.6 - 0.8 based on the maturity of the technology and the reference year for the cost calculation. For most mature technologies, the exponent is expected to be 0.6 while for new equipment and technologies the exponent can be considered as 0.8 [64].

There is usually a limit on the maximum size of equipment. In case the required size of equipment exceeds the limit, multiple trains of the same equipment are installed such that none of the trains exceed the upper limit. For multiple trains of the same equipment, the following equation is used to calculate the cost of the equipment:

$$C_m = C * n^m \quad (4.7)$$

In this formula, n is the number of trains and m is an exponent which is usually taken as 0.9 [64], [79], [80].

The costs are adjusted for inflation in December 2021 using the Chemical Engineering Plant Cost Indices (CEPCI):

$$Component\ Cost_{year\ y} = Component\ Cost_{year\ x} * \frac{CEPCI_{year\ y}}{CEPCI_{year\ x}} \quad (4.8)$$

After size and inflation adjustment, the costs are further adjusted to include the direct costs such as piping, electrical, utilities, off-sites, equipment erection, buildings, and site preparation. In most literature, these costs are referred to as the Balance of Plant (BOP) cost and are mostly cited along with the reference cost C_o [64]

Furthermore, Indirect Costs (IC) such as engineering, head office, start-up, and contingency are also added to the component cost as these expenses are required for the process's general operation and execution.

The BOP and IC are mostly reported as a percentage of the component cost: therefore, the general equation to calculate the Total Plant Cost (TPC) will be the sum of the component costs, BOP, and IC [81]:

$$TPC = \sum_1^n C + \left(\sum_1^n C * BOP\%\right) + \left(\sum_1^n C * IC\%\right) \quad (4.9)$$

In the end, Interest During Construction (IDC) which is usually assumed to be 10 % of the Total Plant Cost (TPC) is used to calculate the Total Plant Investment (TPI) [82].

$$TPI = TPC * (1 + IDC) \quad (4.10)$$

Table 4.12 References for calculating capital costs

Component	CSP	S_o	C_o	f	BOP %	IC %	IDC %	Ref. year	Ref.
Civil works	Feed MW_{th}	300	12.8 M€	0.85	30	Incl.	10	2010	[65]
Feedstock handling	Feed MW_{th}	157	5.3 M€	0.31	10	Incl.	10	2010	[65]
Biomass belt dryer	Water evap kg/sec	0.34	1.9 M€	0.28	10	Incl.	10	2010	[65]
CFB	Dry biomass kg/sec	17.8	18.9 M€	0.75	30	50	15	2010	[65]
Fabric filter	Syngas cum/sec	15.60	0.068 M$	0.60	270	110	5	2002	[83]
RME scrubber	Syngas kmol/sec	1.45	5.2 M€	0.67	30	Incl.	15	2010	[65]
Amine scrubber	Syngas kmol/sec	1.45	5.2 M€	0.67	30	Incl.	15	2010	[65]
Zinc guard bed	Syngas cum/sec	8	0.024 M€	1.00	Incl.		5	2002	[26]
Syngas comp	Comp Work MW_e	10	5 M€	0.67	30	Incl.	15	2010	[65]
CO2 comp	Comp Work MW_e	10	5 M€	0.67	30	Incl.	15	2010	[65]
WGS reactor	$CO+H_2$ kmol/hr	8819	12.2 M€	0.65	Incl.		5	2002	[26]
Rectisol	Syngas Nm^3/hr	200000	56.7 M€	0.63	30	15	15	2010	[65], [79]
FT reactor (with HX)	Syngas cuft/hr	2520000	13.6 M$	0.75	35	32	5	2007	[79]
ATR	$Syngas_{out}$ kmol/hr	31000	93.66 M$	0.90	35	32	5	2007	[79]
HC recovery - distillation	Crude lb./hr	14440	0.72 M$	0.70	35	32	5	2007	[79]
ASU	O_2 kg/sec	31.5	45.5	0.67	Incl.		5	2011	[84], [85]

An additional 10% overhead cost is assumed to include the capital costs of smaller equipment such as small compressors (for pressure loss makeup), pumps, and heat exchangers.

The annual capital cost is calculated by multiplying the Total Plant Investment (TPI) with the annuity factor or Capital Recovery Factor (CRF):

$$Annual\ Capital\ Cost = TPI * CRF \quad (4.11)$$

where CRF is the ratio of a constant annuity to the present value of receiving that annuity for a particular period. The capital recovery factor is computed as follows using discount rate r and the economic lifetime of the plant T:

$$CRF = \frac{r}{1-(1-r)^{-T}} \quad (4.12)$$

4.5.1.2 Operations and Maintenance (O&M) Cost

The O&M cost is broken down into:

- Personal costs
- Maintenance and insurance costs
- Catalysts and chemicals costs
- Oxygen carrier cost

The annual personal costs, maintenance, and insurance costs, and catalysts and chemicals costs are taken as 0.5 %, 2.5 %, and 1 % of the Total Plant Cost (TPC) respectively Hannula et al. (2016) [36], [65]. The annual catalysts and chemical costs are taken as 2 % of TPC for sour WGS reactor as the catalysts for sour WGS reactions are much more expensive than the catalysts for sweets WGS reactions. The annual oxygen carrier cost is always assumed to be 1 % of the TPC.

4.5.1.3 Energy Cost

The annual biomass and electricity costs are calculated as per the assumed annual operating hours and prices for biomass and electricity as well as the respective energy demands (as given in Table 4.10) which can be taken from the model.

4.5.2 Revenue

The product from the BtL plant is sold in the market assuming that the distillate cuts of FT crude from CDU can be sold in the market directly as final fuel products without any post treatment. Since compared to crude oil FT crude is free from sulphur, nitrogen and heteroatom, and require fewer units as per de Klerk (2006) [86], therefore the distillate cut from CDU can be assumed to be the final product. Moreover, any surplus heat from the plant can also be sold to any kind of co-generation unit such as a district heating (DH) supplier. The average fuel prices for March 2022 are given in Table 4.13.

Table 4.13 Fuel prices

Fuel	Price	Unit	Notes
Lighter Hydrocarbon Gas	5.217	$/MMBTU	Price from tradingeconomics.com for 24th March 2022 [87]
Gasoline	8.547	$/gallon	Price from GlobalPetrolPrices.com (Sweden) for 21st March 2022 [88]
Kerosene (Jet A Fuel)	144	$/bbl	Price from IATA.org (Europe and CIS) for 18th March 2022 [89]
Diesel	10.27	$/gallon	Price from GlobalPetrolPrices.com (Sweden) for 21st March 2022 [88]

Wax	1000	$/tonne	Price from paraffinwaxco.com [90]

The revenue from the fuel is calculated using the production of a specific fuel in the Aspen Plus model and the respective fuel price. The surplus heat available is calculated using a utility composite curve. The revenue from surplus heat is calculated using the assumed price of 1 €/GJ.

4.5.3 Economic Parameters

The techno-economic analysis for different configurations and conditions has been discussed and compared based on the following economic parameters.

4.5.3.1 Levelized Cost of Fuel

The Levelized Cost of Fuel (LCOF) is the minimum price that the product (fuel) should be sold at for the investment to be breakeven (no loss and no profit). If the product is sold at a higher price, the project is profitable. If the product is sold at a lower price, there is no net cash inflow and there is a net loss. The Levelized Cost of Fuel (LCOF) is calculated as follows:

$$LCOF\left(\frac{\$}{GJ}\right) = \frac{F + C + E + O - R}{P} \quad (4.13)$$

where F, C, E, O, and R are the annual cost of biomass, annual capital cost, annual electricity cost, annual O&M costs, and annual plant revenue respectively in $ whereas P is the annual energy production of the fuel in GJ.

4.5.3.2 Annual Profit

Annual Profit is the difference between total annual revenue and total annual cost:

$$Annual\ Profit\ (\$) = Annual\ Plant\ Revenue - Annual\ Plant\ Cost \quad (4.14)$$

4.5.3.3 Payback Period

The payback period is an estimate of the number of years it takes for the investment to reach breakeven:

$$PBP\ (yrs) = \frac{Total\ Plant\ Investment}{Annual\ Profit} \quad (4.15)$$

5 Results and Discussion

This chapter includes the validation of the model with the experimental work from literature followed by the model results and the sensitivity analysis along with discussion.

5.1 Validation

CLG sub-model has been evaluated and validated based on experimental data from Condori et al. [22] for the gasification of biomass (olive stone) in a 1.5kW_{th} unit using LD slag as an oxygen carrier. Although the fuel is different compared to the biomass used in this study, it is expected that the fuel conversion would be similar, independent of the type of biomass. The issues could be more related to operations, where the ash fractions and compositions could vary.

Table 5.1 shows the model validation results. An acceptable deviation of the model results and experimental results have been observed.

Table 5.1 Model Validation

	FR Temperature (C)	**λ**	**S/B***	**H_2**	**CO**	**CO_2**	**CH4**	**H_2/CO**	**CGE (%)**
Experimental	930 ± 1	0.26	0.78	38.7	26.3	27.6	6.6	1.47	73.2
Modeling	930 ± 0.1	0.268	0.783	37.1	27.1	28.4	7	1.37	69.5
Difference (%)		-3.1	-0.4	4.1	-3.0	-2.9	-6.06	6.8	5.05

**The definition is as per given in* [22]

5.2 Chemical Looping Gasification

Table 5.2 shows the change in λ by varying the steam to biomass ratio for the base case model where the fuel was forest residue, the fuel reactor was maintained at 935℃ and the steam temperature was maintained at 500 ℃. By increasing the steam flow into the gasifier, the heat required to maintain the gasifier at 935℃ increases. This means more oxygen is required for combusting volatiles to provide heat for autothermal CLG operation, hence λ increases.

Table 5.2 Oxygen to fuel ratio trend with varying steam to biomass ratio

Steam to biomass ratio	**0.65**	**0.7**	**0.8**	**0.9**	**1**	**1.2**
λ	0.369	0.372	0.377	0.381	0.387	0.396

Figure 5.1 shows the trend in the composition of dry and N_2-free syngas with changes in the steam to biomass ratio.

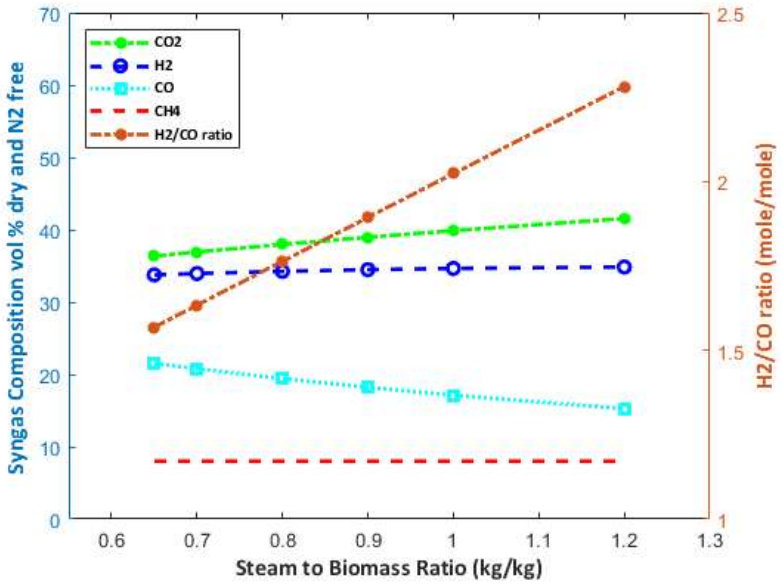

Figure 5.1 Syngas composition and H2/CO ratio by varying steam to biomass ratio

By increasing the steam to biomass ratio, due to water gas shift reaction, H_2 and CO_2 is produced by consuming CO and H_2O. Figure 5.1 also shows increasing trends for H_2 and CO_2 and a decreasing trend for CO, similar to what has been reported by Condori et al. [22].

It is observed that H_2 does not increase in concentration as sharply as CO_2 by providing more steam to the gasifier. The reason for this observation was investigated by changing the gasification agent (steam) temperature. Figure 5.2 shows the trend in the H_2, CO, and CO_2 concentration in the syngas for the steam temperatures of 500 °C and 935 °C.

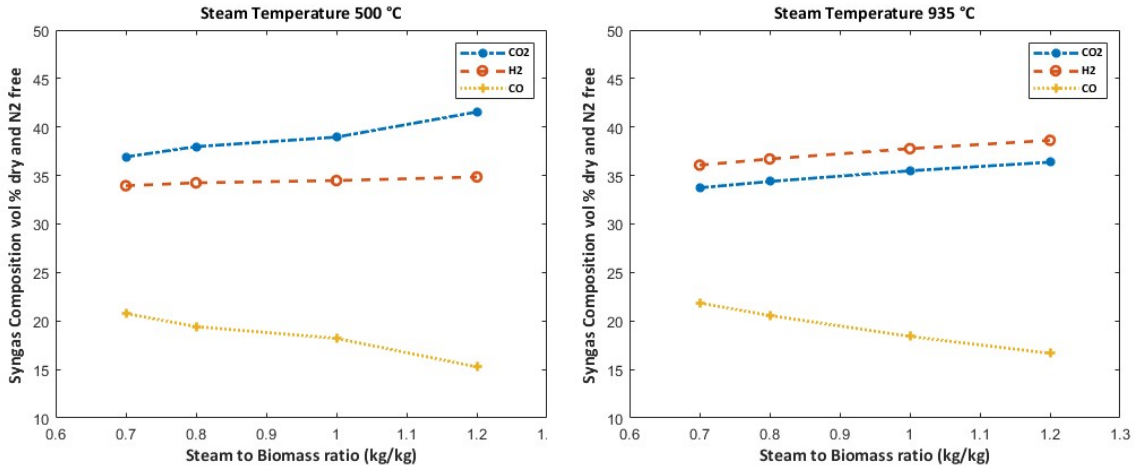

Figure 5.2 Syngas composition by varying steam to biomass ratio for different steam temperatures

The comparison between the two graphs indicates the effect of the gasification agent on the H_2, CO, and CO_2 concentration. The gasifier operates at 935 °C, which is higher than the temperature of steam entering the gasifier (500 °C). This means that by increasing the steam

to biomass ratio, more heat is required for the gasifier to operate at 935°C, which would require more combustion of the syngas, thus converting CO to CO_2 and H_2 to H_2O. Hence, steeper changes in CO and CO2 are observed compared to H_2 as CO converts into CO_2 because of water gas shift reaction and the combustion, whereas there is an increase in H_2 concentration due to water gas shift reaction but some of it gets combusted to H2O. This is also evident from the table above where λ increases as a result of increasing the steam to biomass ratio meaning that more volatiles are burned in the fuel reactor when the steam supply is increased to maintain the fuel reactor temperature at 935 °C.

5.3 Effect of different oxygen carriers

For both LD slag and Ilmenite as oxygen carriers, the model was run for different steam to biomass ratios. Syngas composition, H_2/CO ratio, cold gas efficiency, and fuel production trends for different steam to biomass ratios can be seen in Figure 5.3.

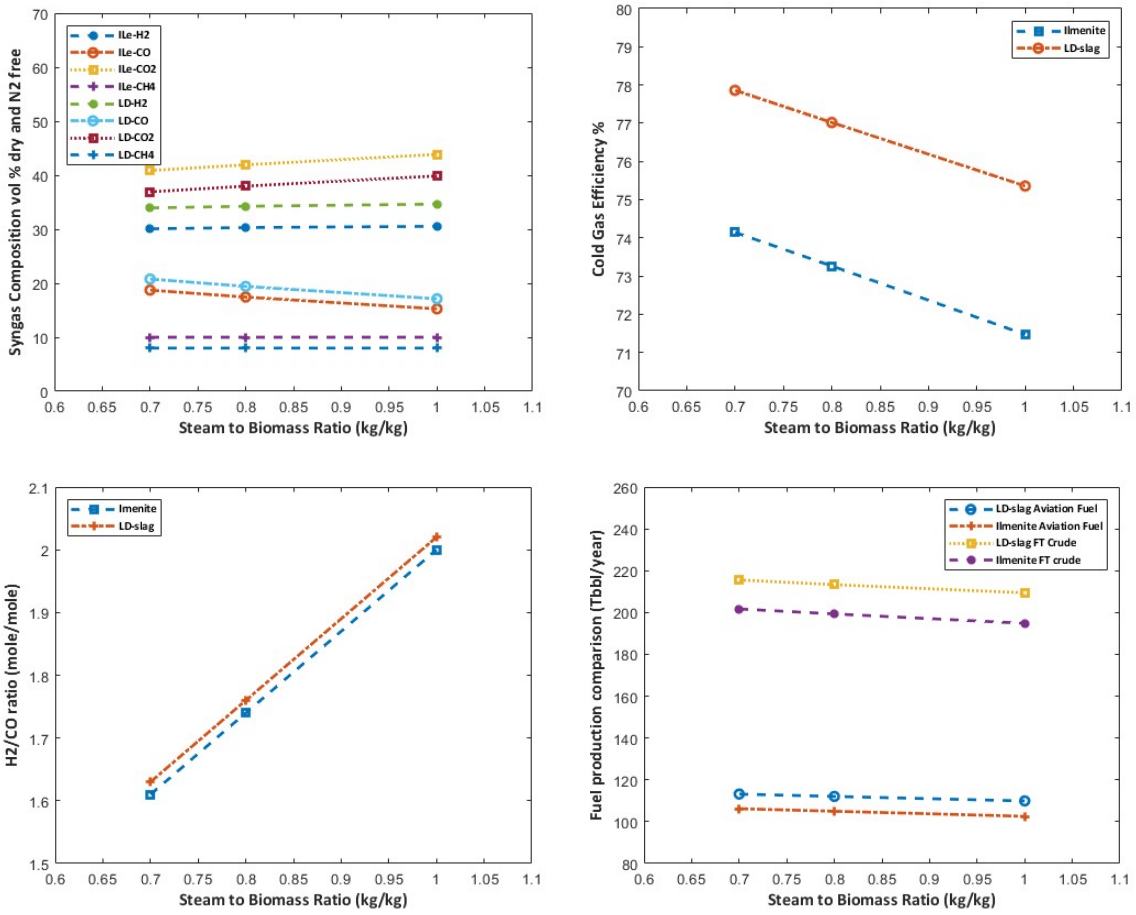

Figure 5.3 Results for LD slag and Ilmenite

The comparison shows that the LD slag produces more syngas and less CO_2 than Ilmenite which is preferable as more CO_2 would mean lower heating value and a higher cost for the CO_2 capture unit. The calcium oxides present in the LD-slag work as a catalyst for the water gas shift reaction resulting in a higher H_2/CO ratio which is more favorable for the Fischer-Tropsch synthesis where an H_2/CO ratio of 2.1 is preferred.

5.4 Techno-economics

The techno-economic results for the base case with LD slag and Ilmenite as an oxygen carrier will be discussed here. The overall economic investigation of bio-jet fuel production needs an estimate of how much a greenfield plant will cost and check the financial indicators, such as payback period, annual profit, and the Levelized Cost of Fuel (LCOF). The Total Plant Investment (TPI) anticipation for the bio-jet fuel can be seen in the table below in which all the equipment and cost are found based on literature and explained in the methodology.

Table 5.3 Total Plant Investment

	Investment (M$)	
Unit	**LD Slag**	**Ilmenite**
Civil works	8.39	8.39
Feedstock handling	7.79	7.79
Biomass belt dryer	6.84	6.84
Indirect Gasifier	43.70	43.70
Fabric filter	0.78	0.77
RME scrubber	5.91	5.85
Amine scrubber	3.93	3.79
Zinc guard bed	0.0036	0.0033
Syngas compressor	6.55	6.31
CO2 compressor	1.63	1.67
Water gas shift reactor	3.45	3.16
Rectisol	7.65	7.34
FT reactor (with HX)	2.21	2.13
ATR	9.62	9.87
HC recovery (distillation)	1.01	0.96
ASU	6.74	6.99
Overhead Cost	11.62	11.56
Total Plant Investment	127.89	127.21

It can be seen in Figure 5.4 and Figure 5.5 that the biggest proportion of the Total Plant Investment (TPI) is the Indirect Gasifier (gasifier used in CLG). It is the same in the paper by Heyne and Harvey (2014) [83] and Roshan et al. (2022) [85]. The difference in component costs between LD slag and Ilmenite as oxygen carrier comes after the chemical looping gasification (indirect gasifier) due to different syngas composition and mass flow in the gasifier for the two different oxygen carriers. As seen in Figure 5.3, LD slag has better syngas production in terms of molar flow/volumetric flow, leading to larger components post gasification. This is also evident from the cost comparison between different units for LD slag and Ilmenite given in Table 5.3.

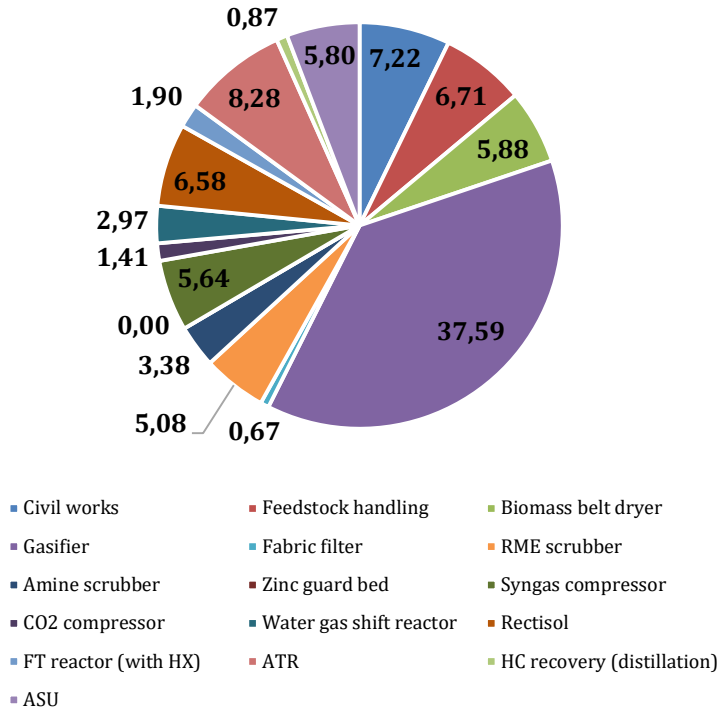

Figure 5.4 Share of TPI (%) - LD Slag

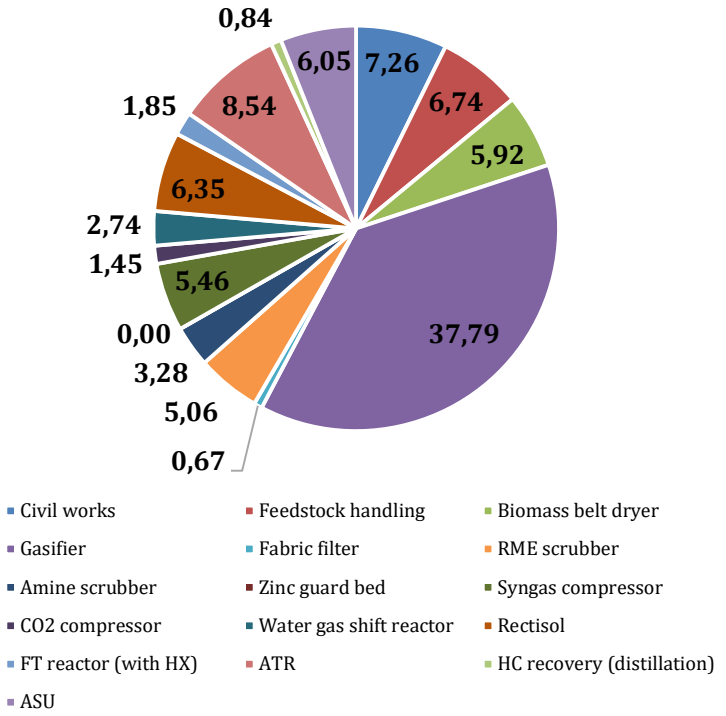

Figure 5.5 Share of TPI (%) - Ilmenite

The overall techno-economic analysis can be seen in Table 5.4.

Table 5.4 Process/Techno-economic Parameters

Techno-economic Parameters	LD Slag	Ilmenite
Cold Gas Efficiency (%)	77.67	73.95
Conversion Efficiency - BtL (%)	39.76	37.14
Higher Heating Value of FT crude (MJ/kg)	45.83	45.73
Mass flowrate of FT crude (kg/sec)	0.76	0.71
Energy Content of FT crude - Based on HHV (MW)	35.01	32.69
CO2 captured (kg/sec)	5.35	5.53
Annual Capital Cost (M$/yr)	15.53	15.45
Annual O&M Cost (M$/yr)	5.37	5.35
Annual Electricity Cost (M$/yr)	7.06	6.45
Annual Biomass Cost (M$/yr)	11.33	11.33
Total Annual Cost (M$/yr)	39.31	38.59
Annual Revenue - DH (M$/yr)	0.28	0.34
Natural Gas Production (lb/hr)	53.54	51.90
Gasoline Production (gallon/hr)	240.17	221.60
Jet Fuel Production (bbl/hr)	14.05	13.20
Diesel Production (gallon/hr)	152.78	143.71
Wax Production (tonne/hr)	0.22	0.20
Annual Revenue – CDU products (M$/yr)	46.99	43.89
Total Annual Revenue (M$/yr)	47.28	44.23
Levelized Cost of Fuel - LCOF ($/GJ)	38.71	40.61
Annual Profit (M$/yr)	7.96	5.64
Payback Period (yrs)	16.60	23.30
Excess Heat available to sell for DH (MW)	9.07	10.99

Although the total costs for the plants with LD slag and Ilmenite as oxygen carriers are almost the same, there is a considerable difference in the syngas and FT crude production (evident from the differences in cold gas and conversion efficiencies). LD slag has better syngas production leading to better FT crude production and ultimately, better economic performance as seen in Table 5.4. The annual revenue from the CDU products for LD slag as oxygen carrier is 6.8 % higher than that with Ilmenite. Using LD slag as OC, leads to 41 % higher annual cash flow compared to Ilmenite. Although the model with Ilmenite as OC has more excess heat available, but since the heat is of low value, it doesn't affect the technoeconomic analysis much.

5.5 Different carbon capture technologies and configurations

This chapter compares and investigates the technoeconomic performance of the BtL processes with CCS technologies and configurations given in Table 4.10.

The economic evaluation of the system was according to the literature review of different cost references and prices for services and all equipment. The techno-economic parameters such as Levelized Cost of Fuel (LCOF), annual profit, jet fuel production, and conversion efficiency were evaluated for all cases in the table above. Figure 5.6 indicates that Case **A** has the highest jet fuel production while Case **C** has the lowest production rate.

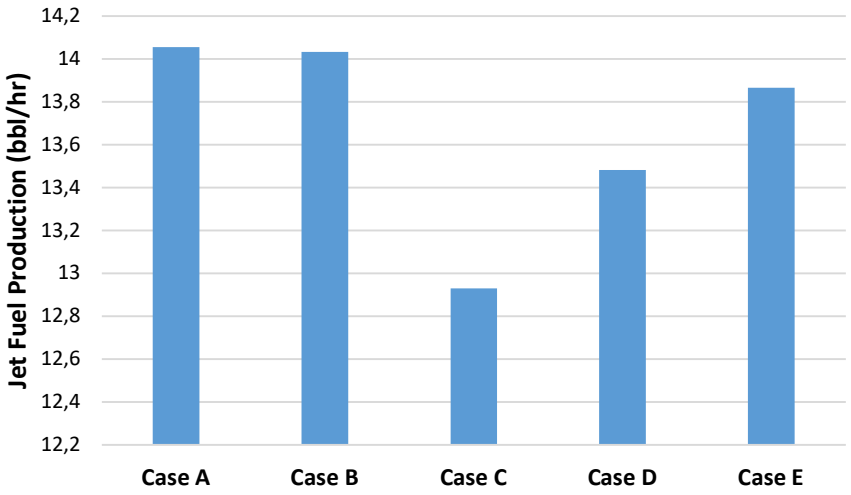

Figure 5.6 Jet Fuel Production

These results are aligned with the chemical efficiency (conversion efficiency) of the biomass to liquid fuel as seen in Figure 5.7. Case **A** has the lowest amount of CO_2 in the Fischer Tropsch Synthesis and Autothermal reformer (ATR) units that will affect the system and fuel production rate while it is the opposite for the system with Case **C** that has the highest CO_2 circulation in the system.

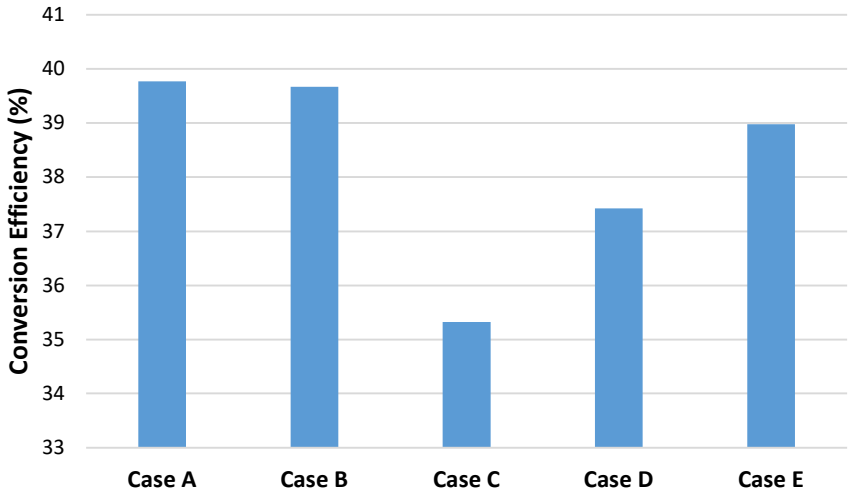

Figure 5.7 Conversion Efficiencies

While the performance indicators suggest Case **A** is the best case among all the configurations, the economic evaluation indicates that Case **E** has the best economic

performance. The Levelized Cost of Fuel (LCOF) for all the cases indicates that the Amine scrubber with 90 % carbon capture efficiency has the lowest production cost as seen in Figure 5.8. The comparison between configurations with Rectisol only (case B) and Amine Scrubber only (cases C, D and E) can be expressed from the standpoint of the cost of the energy for running the plant as there is a greater demand of electricity for the plant configuration with Rectisol only (case B) compared to the plant configuration with only Amine absorber (cases C, D and E). The Rectisol unit needs a lot of electricity, which is expensive while Amine scrubber mostly requires heat which is available in the system. Also, since excess heat is sold very cheaply, the opportunity cost for using heat in Amine scrubber is very small.

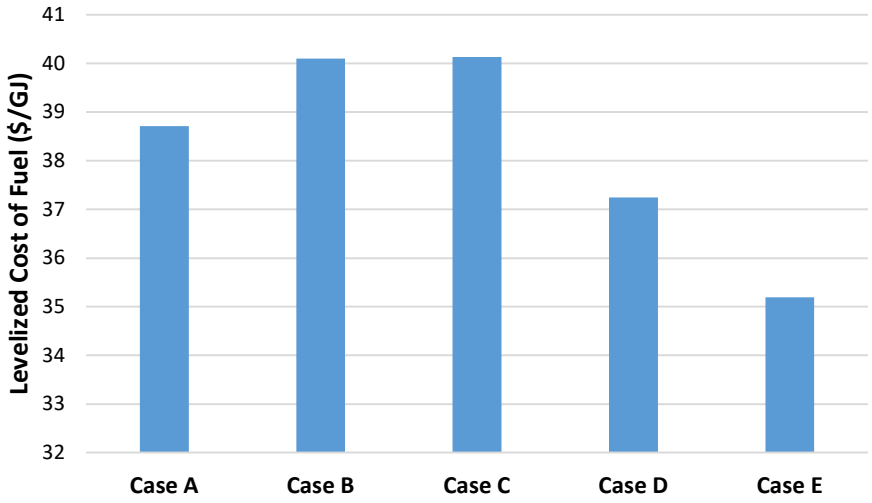

Figure 5.8 Levelized Cost of Fuel

The utility composite curve in Figure 5.9 shows the total excess heat available for the case E which shows that the system can provide enough energy for the carbon capture unit and also sell around 2 MW of heat to district heating network.

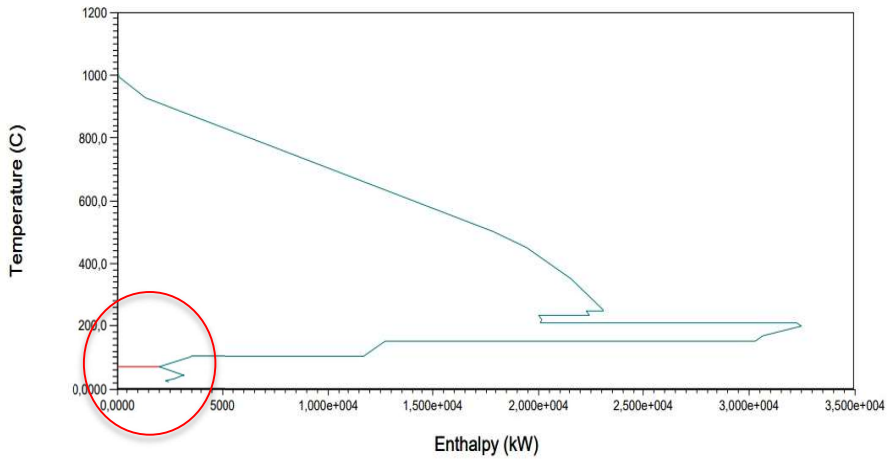

Figure 5.9 Utility Composite Curve for the best-case configuration (case E)

The annual profit of the different configurations also shows that Case **E** is the best configuration among all cases while the first two case with Rectisol unit have the highest fuel production rate.

A comparison with other BtL studies for jet fuel production has been done and it reveals that the Levelized Cost of Fuel (LCOF) for the case with Amine scrubber (with 90 % efficiency) is 20-28 % cheaper than other similar studies for similar biofuels in Table 5.5.

Table 5.5 Technoeconomic comparison with other BtL processes

	Most economic case (Case E)	**M. Li et al.** [91]	**I. S. Tagomori** [92]	**Roshan et al.** [85]
Levelized cost of FT crude	110 €/MWh	124–141 €/MWh	125-130 €/MWh	119-138 €/MWh

Techno-economic analysis by Roshan et al. (2022) [85] is a simplistic one estimating the cost of FT crude only whereas this study estimates both the costs and the revenues to calculate the annual cash inflow for the project. Since syncrude needs a lesser number of units for refining compared to crude oil as per de Klerk [86] and also on average between 130 % to 189 % more valuable than conventional crude oil as per Michael J. Gradassi , the LCOF of syncrude is not compared with the current crude oil price in the market as done in Roashan et al. (2022) [85], rather we distill syncrude to produce aviation fuel along with other valuable byproducts, sell them to generate revenue and estimate the annual cash inflow. Based on the assumptions done in the techno-economic analysis, it is predicted that there is an annual cash inflow/profit even without any CO_2 tax credit.

5.6 Sensitivity Analysis

Several sensitivity analyses have been done on the performance of the best case BtL model and carbon capture configuration (Case **E**) on several points on the Fischer-Tropsch synthesis and CLG unit. The analyses were done on the Fischer-Tropsch synthesis reactor temperature, water gas shift reactor steam temperature, steam to biomass ratio in the fuel reactor, and the fuel moisture content.

5.6.1 FT reactor temperature

The FT reactor temperature was changed between 200-240 °C and the model was checked for the conversion efficiency, levelized cost of fuel, and the jet fuel production. As it showed in Figure 5.10, if the FT reactor temperature decreases the conversion efficiency of the system also decreases. This is because at higher FT temperatures, the fraction of hydrocarbons with lower carbon number in the FT reactor outlet stream is higher. These shorter hydrocarbons have lower boiling points meaning that more hydrocarbons recirculate and go through the ATR unit which decreases the mass flow of FT crude and hence the conversion efficiency.

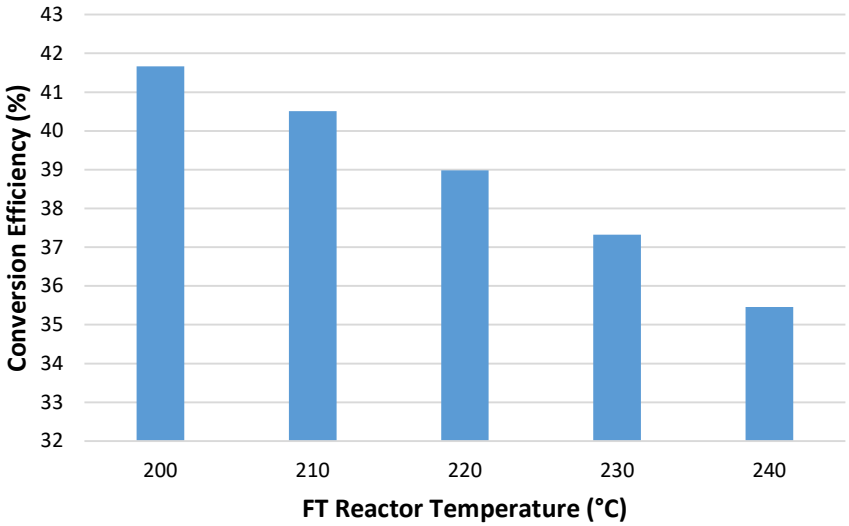

Figure 5.10 Conversion efficiencies for different FT reactor temperatures

It can be seen in Figure 5.11 that the levelized cost of fuel (FT crude) increases by increasing the FT reactor temperature. The reason for this is the low fuel production from the plant at higher FT temperatures.

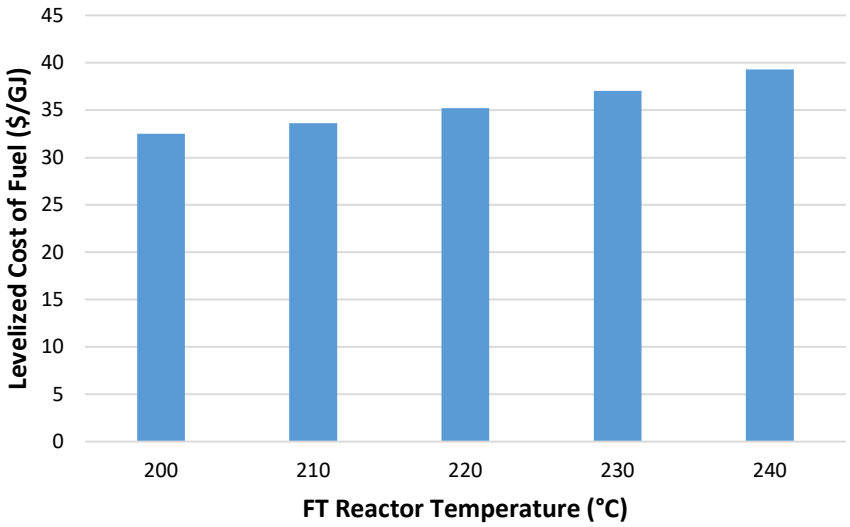

Figure 5.11 Levelized Cost of Fuel

However, for jet fuel production the best temperature is around 220 °C in FT synthesis which result in the highest fuel production rate. A comparison between temperatures shows a peak at 220 °C as seen in Figure 5.12.

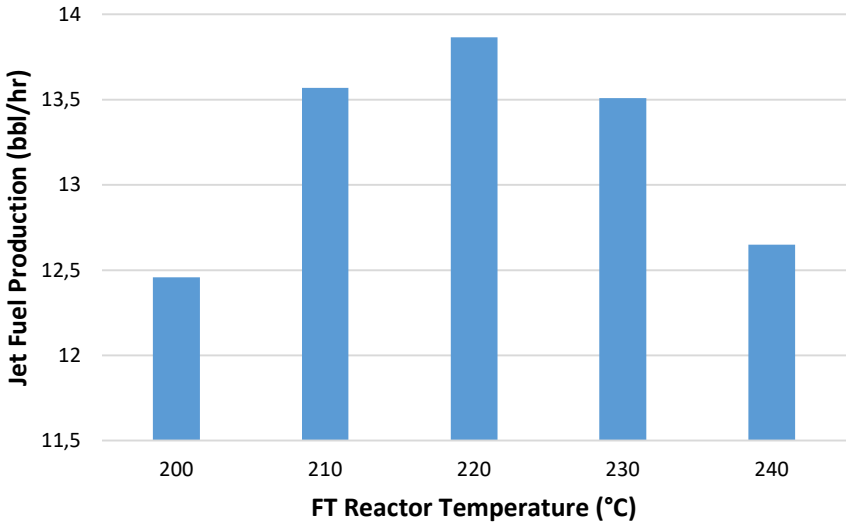

Figure 5.12 Jet fuel production for different FT reactor temperatures

The annual profit for the system follows the conversion efficiency as most of the prices for the products are based on the energy content of the fuel, consequently, the lower temperature will have higher profitability. However, in this study the aim is to maximize jet fuel production, therefore the best temperature for FT will be based on the fuel production rate which is 220 °C in this case.

5.6.2 Water-gas shift reactor temperature

A study was done for checking the effect of the WGS reactor temperature on the plant process parameters, in which it was found that there was no significant change in the plant parameters. The result for conversion efficiency and jet fuel production can be seen in Figure 5.13.

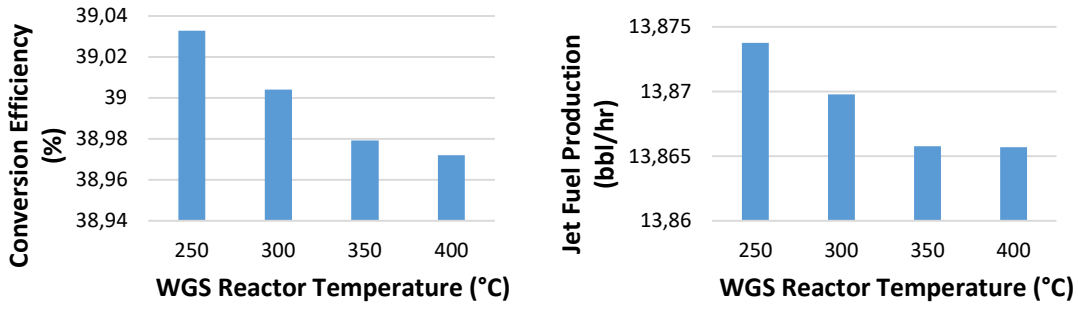

Figure 5.13 Conversion efficiency and jet fuel production comparison for different WGS reactor steam temperature

It can be observed that by increasing the temperature from 250 to 400 °C the conversion efficiency and jet fuel production change only slightly, which indicates a negligible effect of WGS reactor temperature on the overall process.

5.6.3 Steam to biomass ratio

Figures 5.1 and 5.14 show the variations in the composition of syngas from the CLG unit by varying the steam to biomass ratio. By increasing the steam to biomass ratio, more the water gas shift reaction happens converting more CO to form more H_2 and CO_2 and increasing the H_2/CO ratio.

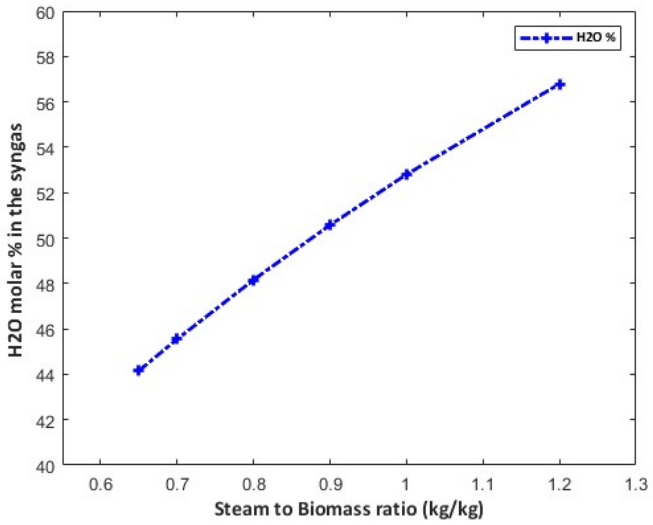

Figure 5.14 H2O concentration in syngas

As steam enters the gasifier at a temperature lower than the gasifier temperature, by increasing the steam to biomass ratio, more syngas needs to be combusted to maintain the gasifier temperature. This is evident from the trend in the excess air ratio λ which increases from 0.369 to 0.396 by increasing the steam to biomass ratio from 0.65 to 1.2 which indicates that more syngas is combusted in the gasifier converting CO to CO_2 and H_2 to H_2O, hence justifying a sharper increase in CO_2 composition compared to that of H_2. The figure shows that the H_2O composition also increases by increasing the steam to biomass ratio meaning that not all the steam goes through water gas shift reaction.

The steam to biomass ratio also effects the cold gas efficiency and the chemical efficiency of the plants which is presented in Figure 5.15, it shows that by increasing the steam to biomass ratio the efficiencies will drop and the fuel production will also drop accordingly.

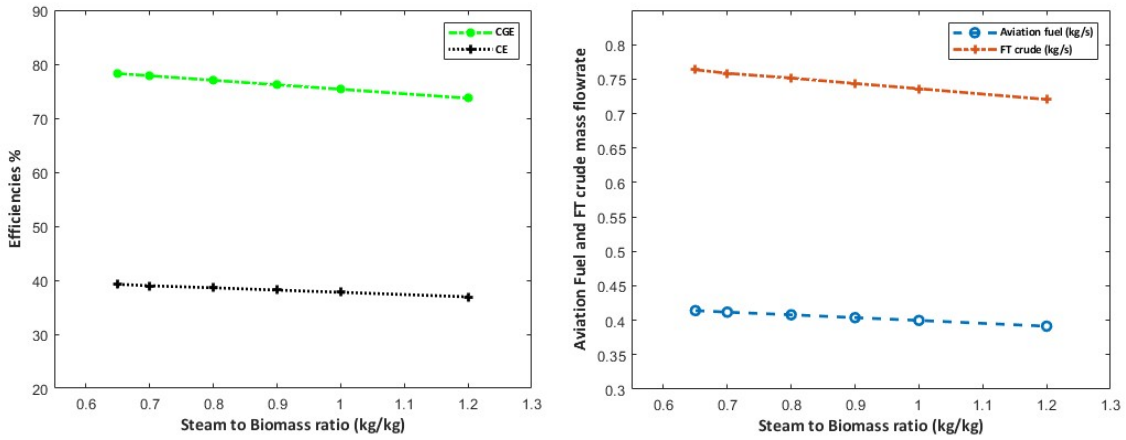

Figure 5.15 S/B effect on process efficiencies and fuel production

5.6.4 Biomass moisture content after drying

The study on the moisture content of the biomass shows that it is one of the most significant metrics affecting the process performance. As expected, the results in Figure 5.16 show that the best cold gas and conversion efficiencies are for the lowest biomass moisture contents. A moisture level of more than 30% might make gasifier ignition difficult and diminish the calorific value of the produced gas significantly [56].

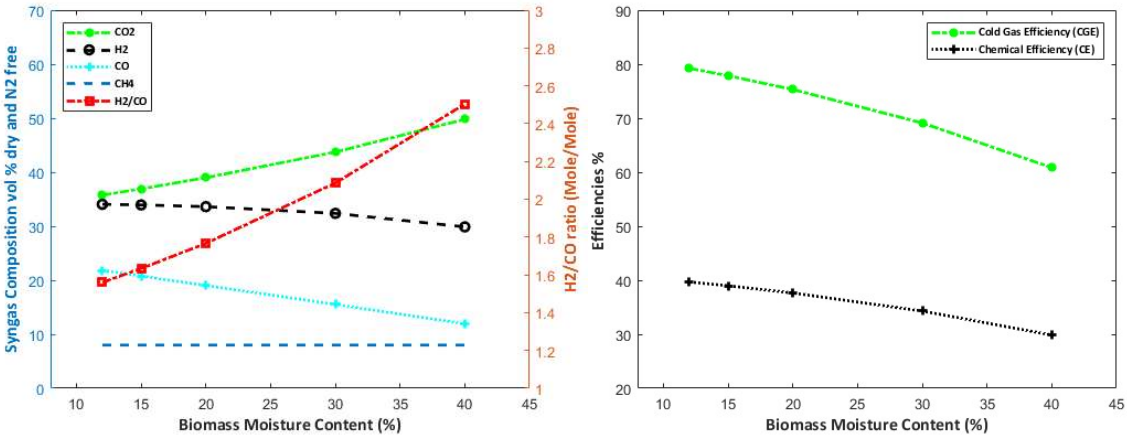

Figure 5.16 Biomass moisture effect on Syngas composition and efficiencies

Increasing the extent of the WGS reaction leads to increased H_2 production at the cost of CO composition in the syngas leading to higher H_2/CO ratios. Also, since the heat of combustion of H_2 is less than the heat of combustion of CO, the net calorific value of the syngas drops which is also observed in the literature [56]. However, for higher moisture contents, more H_2 gets combusted to keep the gasifier temperature constant because the moisture cools down the gasifier resulting in a greater heat demand which comes from combusting syngas (H_2 + CO). In other words, apart from the WGS reaction which consumes CO and produces H_2, CO and H_2 are also consumed due to the combustion of syngas resulting in a drop in H_2 concentration as well.

For the best economical case (Case E) with a steam to biomass ratio of 0.7, a sensitivity analysis for biomass moisture content such that the gasifier load (based on LHV of biomass) is kept constant shows a drop in the cash inflow (annual profit) of the plant. This is because, maintaining the gasifier load with a biomass that has a higher moisture content requires a greater flow of biomass. This has two consequences:

- First, there is a need for a larger gasifier since the gasifier is sized based on the flow rate of biomass entering the gasifier.
- Second, a higher biomass flow entering the gasifier requires a greater steam flow into the gasifier for a constant steam to biomass ratio leading to poor process efficiencies.

Figure 5.17 shows a drop in annual profit with increasing biomass moisture contents. At 40 % moisture content, the annual profit gets negative meaning there will be no cash inflow and the project will be economically infeasible.

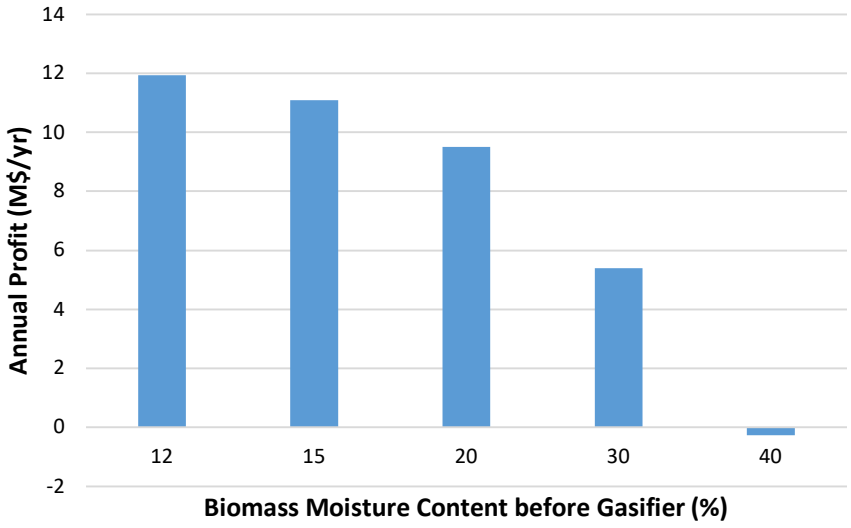

Figure 5.17 Annual profits with varying biomass moisture content

6 Conclusion

This study models the full chain BtL process using Aspen Plus software. The model is designed for a biomass supply of around 80 MW_{th} and includes drying of biomass followed by a CLG unit using LD-slag and Ilmenite as the oxygen carriers. The circulation rates of oxygen carriers are adjusted to achieve the desired syngas temperature of 935°C in the fuel reactor (FR). The resulting syngas from CLG goes through syngas cleaning and conditioning units to meet the requirements for FT synthesis. In the FT reactor, the syngas gets converted into hydrocarbons with carbon numbers ranging from 1 to 40 using the Anderson-Schulz-Flory distribution. Since the aim of the model is to produce aviation fuel, the FT synthesis process combined with a reformer in the recycle loop is adjusted for maximizing the yield of paraffin with carbon numbers ranging from 8 to 16.

A comprehensive comparison of the process parameters between LD-slag and Ilmenite as oxygen carriers for Chemical Looping Gasification has been presented in this study which was validated with the experimental studies done by Condori et al. (2021). Moreover, sensitivity and technoeconomic analysis for different process parameters and plant configurations have also been carried out. The study shows that the LD-slag has a better syngas yield with less CO_2 gas than Ilmenite, resulting in a better cold gas efficiency. This is due to calcium oxides present in LD slag acting as a catalyst for the water gas shift reaction resulting in H_2/CO ratio close to that required for FT synthesis (∼2.1). The techno-economic evaluation of the systems shows that the CLG unit is the most expensive equipment in the process and accounts for almost one-third of the whole system cost. Increasing the moisture content in the biomass entering the gasifier or the steam to biomass ratio for the gasifier, both result in drop in process efficiencies ultimately leading to poor technoeconomic performances.

As per the optimized model (case E), the clean syngas produced by the syngas cleaning unit has a cold-gas efficiency of 77.86% and a heating value of 8.68 MJ/Nm3 (LHV base). The FT synthesis model with a reformer shows that 647 bbl/day of FT crude will be produced, with 154 kilo tonne of CO2 being captured annually and a conversion efficiency of 38.98% from biomass to FT-crude. The computed levelized cost of fuel (LCOF) for FT crude is 35.19 $ per GJ, with an annual plant profit (cash inflow) of 11.09 M$ and an initial investment payback period of 11.56 years.

The conventional processes downstream of the CLG unit consist of two separate CO2 capture units which increase the capital cost of the BTL production; therefore, by altering different configurations for CO_2 units in the process and doing a technoeconomic comparison, the most profitable configuration was found to be the one with amine absorber only (with 90% carbon capture efficiency). The cascade analysis of the process streams showed that there was always enough heat to provide for the CO_2 capture unit with surplus heat sold to the district heating network. FT reactor temperature of 220 °C is the most optimal for maximizing the production of aviation fuel. Higher FT temperature resulted in production of more natural gas and gasoline whereas lower temperatures resulted in better yields of diesel and waxes, both at the cost of jet fuel yield. There was no significant impact on the process and economic parameters of the plant by varying the WGS reactor temperature.

7 References

[1] S. Solomon, *Climate change 2007 : The Physical Science Basis (Contribution of Working Group I to the Fourth Assessment Report of the Intergovernmental Panel on Climate Change)*. Cambridge University Press, 2007.

[2] Henrik Thunman, *GoBiGas demonstration-a vital step for a large-scale transition from fossil fuels to advanced biofuels and electrofuels*. Accessed: Sep. 13, 2022. [Online]. Available: https://www.chalmers.se/SiteCollectionDocuments/SEE/News/Popularreport_GoBiGas_results_highres.pdf

[3] Hannah Ritchie, "Cars, planes, trains: where do CO2 emissions from transport come from?" https://ourworldindata.org/co2-emissions-from-transport (accessed Dec. 06, 2020).

[4] Stephen Arrowsmith, David S Lee, Jasper Faber, and Lisanne van Wijngaarden, "Updated analysis of the non-CO2 climate impacts of aviation and potential policy measures pursuant to the EU Emissions Trading System Directive Article 30(4)," Brussels, 2020.

[5] Unfccc, "ADOPTION OF THE PARIS AGREEMENT - Paris Agreement text English," 2015. Accessed: Mar. 28, 2022. [Online]. Available: https://unfccc.int/process-and-meetings/the-paris-agreement/the-paris-agreement

[6] V. Masson-Delmotte *et al.*, "Global warming of 1.5°C: An IPCC special report on the impacts of global warming of 1.5°C," 2019. [Online]. Available: www.environmentalgraphiti.org

[7] T. Gasser, C. Guivarch, K. Tachiiri, C. D. Jones, and P. Ciais, "Negative emissions physically needed to keep global warming below 2°C," *Nat Commun*, vol. 6, Aug. 2015, doi: 10.1038/ncomms8958.

[8] S. v Hanssen, V. Daioglou, Z. J. N. Steinmann, J. C. Doelman, D. P. van Vuuren, and M. A. J. Huijbregts, "The climate change mitigation potential of bioenergy with carbon capture and storage," *Nat Clim Chang*, vol. 10, no. 11, pp. 1023–1029, 2020, doi: 10.1038/s41558-020-0885-y.

[9] Mikko Hupa and Maria Zevenhoven, "Fluidised Bed Conversion," Turku, Finland, 2003.

[10] Henrik Thunman, "combustion Engineering," *DEPARTMENT OF ENERGY AND ENVIRONMENT CHALMERS UNIVERSITY OF TECHNOLOGY*, 2020.

[11] G. Aranda, A. A. van der Drift, B. J. Vreugdenhil, H. J. M. Visser, C. F. Mourao, and V. C. M. van der Meijden, "Comparing direct and indirect fluidized bed

gasification: Effect of redox cycle on olivine activity," 2013, doi: 10.1002/ep.12016.

[12] E. Sette, D. Pallarès, and F. Johnsson, "Influence of bulk solids cross-flow on lateral mixing of fuel in dual fluidized beds," *Fuel Processing Technology*, vol. 140, pp. 245–251, 2015, doi: https://doi.org/10.1016/j.fuproc.2015.09.017.

[13] J. Dai and K. J. Whitty, "Chemical looping gasification and sorption enhanced gasification of biomass: A perspective," *Chemical Engineering and Processing - Process Intensification*, vol. 174, p. 108902, 2022, doi: https://doi.org/10.1016/j.cep.2022.108902.

[14] A. Lyngfelt and B. Leckner, "A 1000 MWth boiler for chemical-looping combustion of solid fuels – Discussion of design and costs," *Appl Energy*, vol. 157, pp. 475–487, Nov. 2015, doi: 10.1016/j.apenergy.2015.04.057.

[15] M. Ishida, D. Zheng, and T. Akehata, "EVALUATION OF A CHEMICAL-LOOPING-COMBUSTION POWER-GENERATION SYSTEM BY GRAPHIC EXERGY ANALYSIS," 1987.

[16] N. M. Nguyen, F. Alobaid, P. Dieringer, and B. Epple, "Biomass-based chemical looping gasification: Overview and recent developments," *Applied Sciences (Switzerland)*, vol. 11, no. 15. MDPI AG, Aug. 01, 2021. doi: 10.3390/app11157069.

[17] T. Mendiara, A. Abad, L. F. de Diego, F. García-Labiano, P. Gayán, and J. Adánez, "Biomass combustion in a CLC system using an iron ore as an oxygen carrier," *International Journal of Greenhouse Gas Control*, vol. 19, pp. 322–330, 2013, doi: 10.1016/j.ijggc.2013.09.012.

[18] Z. Huang *et al.*, "In-situ removal of toluene as a biomass tar model compound using NiFe2O4 for application in chemical looping gasification oxygen carrier," *Energy*, vol. 190, Jan. 2020, doi: 10.1016/j.energy.2019.116360.

[19] G. Huijun, S. Laihong, F. Fei, and J. Shouxi, "Experiments on biomass gasification using chemical looping with nickel-based oxygen carrier in a 25 kWth reactor," *Appl Therm Eng*, vol. 85, pp. 52–60, Jun. 2015, doi: 10.1016/j.applthermaleng.2015.03.082.

[20] H. Sozen, G.-Q. Wei, H.-B. Li, H. E. Fang, and Z. Huang, "Foundation item: Supported by the National Natural Science Foundation of China (51076154) and the National Key Technology Research & Development Program of 12th Five-year of China (2011BAD15B05)," 2014.

[21] O. Condori, F. García-Labiano, L. F. de Diego, M. T. Izquierdo, A. Abad, and J. Adánez, "Biomass chemical looping gasification for syngas production using ilmenite as oxygen carrier in a 1.5 kWth unit," *Chemical Engineering Journal*, vol. 405, Feb. 2021, doi: 10.1016/j.cej.2020.126679.

[22] O. Condori, F. García-Labiano, L. F. de Diego, M. T. Izquierdo, A. Abad, and J. Adánez, "Biomass chemical looping gasification for syngas production using LD Slag as oxygen carrier in a 1.5 kWth unit," *Fuel Processing Technology*, vol. 222, Nov. 2021, doi: 10.1016/j.fuproc.2021.106963.

[23] A.P.Steynberg and M.E. Dry, *Fisher-Tropsch Technology*, 1st ed., vol. 152. Elsevier, 2004.

[24] A. B. De, L. Ree, L. M. Best, and A. F. Hepp, "Fischer-Tropsch Catalyst for Aviation Fuel Production," 2011.

[25] B. H. Davis, "Overview of reactors for liquid phase Fischer-Tropsch synthesis," 2002.

[26] C. N. Hamelinck, A. P. C. Faaij, H. den Uil, and H. Boerrigter, "Production of FT transportation fuels from biomass; technical options, process analysis and optimisation, and development potential," *Energy*, vol. 29, no. 11, pp. 1743–1771, 2004, doi: 10.1016/j.energy.2004.01.002.

[27] S. Achinas, S. Margry, and G. J. W. Euverink, "8 - A technological outlook of biokerosene production," in *Sustainable Biofuels*, R. C. Ray, Ed. Academic Press, 2021, pp. 225–246. doi: https://doi.org/10.1016/B978-0-12-820297-5.00011-6.

[28] I. Dimitriou, H. Goldingay, and A. v. Bridgwater, "Techno-economic and uncertainty analysis of Biomass to Liquid (BTL) systems for transport fuel production," *Renewable and Sustainable Energy Reviews*, vol. 88. Elsevier Ltd, pp. 160–175, May 01, 2018. doi: 10.1016/j.rser.2018.02.023.

[29] WBA, "THE CARBON NEUTRALITY OF BIOMASS FROM FORESTS," *World Bioenergy Association*, 2013.

[30] S. Y. Searle and C. J. Malins, "Waste and residue availability for advanced biofuel production in EU Member States," *Biomass Bioenergy*, vol. 89, pp. 2–10, Jun. 2016, doi: 10.1016/j.biombioe.2016.01.008.

[31] H. Yang, R. Yan, H. Chen, C. Zheng, D. H. Lee, and D. T. Liang, "In-depth investigation of biomass pyrolysis based on three major components: Hemicellulose, cellulose and lignin," *Energy and Fuels*, vol. 20, no. 1, pp. 388–393, Jan. 2006, doi: 10.1021/ef0580117.

[32] A. Kumar, S. Adamopoulos, D. Jones, and S. O. Amiandamhen, "Forest Biomass Availability and Utilization Potential in Sweden: A Review," *Waste and Biomass Valorization*, vol. 12, no. 1. Springer Science and Business Media B.V., pp. 65–80, Jan. 01, 2021. doi: 10.1007/s12649-020-00947-0.

[33] C. Wang *et al.*, "Utilization of biomass for blast furnace in Sweden-Report I: Biomass availability and upgrading technologies."

[34] L. Radačovská, M. Holubčík, R. Nosek, and J. Jandačka, “Influence of Bark Content on Ash Melting Temperature,” in *Procedia Engineering*, 2017, vol. 192, pp. 759–764. doi: 10.1016/j.proeng.2017.06.131.

[35] Carl. Wilén, Antero. Moilanen, and Esa. Kurkela, *Biomass feedstock analyses*. Technical Research Centre of Finland, 1996.

[36] I. Hannula, “Online supplementary material for Hydrogen enhancement potential of synthetic biofuels manufacture in the European context: A techno-economic assessment,” 2016.

[37] A. Anukam and J. Berghel, “Biomass Pretreatment and Characterization: A Review,” in *Biotechnological Applications of Biomass*, IntechOpen, 2021. doi: 10.5772/intechopen.93607.

[38] Salman Zafar, “Biomass Pelletization Process,” Sep. 2021. https://www.bioenergyconsult.com/biomass-pelletization/ (accessed Aug. 09, 2022).

[39] F. and R. A. O. C. Ministry of Agriculture, “Biomass densification for energy production,” *ISSN 1198-712X*, 2011. https://www.ontario.ca/page/biomass-densification-energy-production (accessed Aug. 09, 2022).

[40] H. Leion, T. Mattisson, and A. Lyngfelt, “Solid fuels in chemical-looping combustion,” *International Journal of Greenhouse Gas Control*, vol. 2, no. 2, pp. 180–193, 2008, doi: 10.1016/S1750-5836(07)00117-X.

[41] M. Jong, Y. J. Lee, J. Kim, S. Lee, and K. Done, “COAL-GASIFICATION KINETICS DERIVED FROM PYROLYSIS IN A FLUIDIZED-BED REACTOR,” 1998.

[42] Z. Cheng, L. Qin, J. A. Fan, and L. S. Fan, “New Insight into the Development of Oxygen Carrier Materials for Chemical Looping Systems,” *Engineering*, vol. 4, no. 3. Elsevier Ltd, pp. 343–351, Jun. 01, 2018. doi: 10.1016/j.eng.2018.05.002.

[43] J. Adánez, A. Abad, T. Mendiara, P. Gayán, L. F. de Diego, and F. García-Labiano, “Chemical looping combustion of solid fuels,” *Progress in Energy and Combustion Science*, vol. 65. Elsevier Ltd, pp. 6–66, Mar. 01, 2018. doi: 10.1016/j.pecs.2017.07.005.

[44] E. Jerndal, T. Mattisson, and A. Lyngfelt, “Thermal analysis of chemical-looping combustion,” *Chemical Engineering Research and Design*, vol. 84, no. 9 A, pp. 795–806, 2006, doi: 10.1205/cherd05020.

[45] P. Dieringer, F. Marx, F. Alobaid, J. Ströhle, and B. Epple, “Process control strategies in chemical looping gasification-A novel process for the production of biofuels allowing for net negative CO2 emissions,” *Applied Sciences (Switzerland)*, vol. 10, no. 12, Jun. 2020, doi: 10.3390/app10124271.

[46] S. Pissot, T. B. Vilches, H. Thunman, and M. Seemann, “Dual fluidized bed gasification configurations for carbon recovery from biomass,” *Energy and Fuels*, vol. 34, no. 12, pp. 16187–16200, Dec. 2020, doi: 10.1021/acs.energyfuels.0c02781.

[47] C. Frilund, S. Tuomi, E. Kurkela, and P. Simell, “Small- to medium-scale deep syngas purification: Biomass-to-liquids multi-contaminant removal demonstration,” *Biomass Bioenergy*, vol. 148, May 2021, doi: 10.1016/j.biombioe.2021.106031.

[48] P. J. Woolcock and R. C. Brown, “A review of cleaning technologies for biomass-derived syngas,” *Biomass and Bioenergy*, vol. 52. pp. 54–84, May 2013. doi: 10.1016/j.biombioe.2013.02.036.

[49] R. Zwart and J. Krogh, “Tar removal from low-temperature gasifiers,” 2010.

[50] A. L. Kohl and R. B. Nielsen, “CHAPTER 7 - Sulfur Dioxide Removal,” in *Gas Purification (Fifth Edition)*, A. L. Kohl and R. B. Nielsen, Eds. Houston: Gulf Professional Publishing, 1997, pp. 466–669. doi: https://doi.org/10.1016/B978-088415220-0/50007-0.

[51] N. Korens, D. R. Simbeck, and D. J. Wilhelm, “PROCESS SCREENING ANALYSIS OF ALTERNATIVE GAS TREATING AND SULFUR REMOVAL FOR GASIFICATION,” 2002. [Online]. Available: www.sfapacific.com

[52] C. Frilund, P. Simell, N. Kaisalo, E. Kurkela, and M. L. Koskinen-Soivi, “Desulfurization of Biomass Syngas Using ZnO-Based Adsorbents: Long-Term Hydrogen Sulfide Breakthrough Experiments,” *Energy and Fuels*, vol. 34, no. 3, pp. 3316–3325, Mar. 2020, doi: 10.1021/acs.energyfuels.9b04276.

[53] A. Kohl and R. Nielsen, “Gas purification,” 1988.

[54] H. Boerrigter, H. den Uil, and H.-P. Calis, “Green Diesel from Biomass via Fischer-Tropsch synthesis: New Insights in Gas Cleaning and Process Design.”

[55] G. Barbieri, “Water Gas Shift (WGS),” in *Encyclopedia of Membranes*, Springer Berlin Heidelberg, 2015, pp. 1–4. doi: 10.1007/978-3-642-40872-4_598-1.

[56] H. A. Choudhury, S. Chakma, and V. S. Moholkar, “Biomass Gasification Integrated Fischer-Tropsch Synthesis: Perspectives, Opportunities and Challenges,” in *Recent Advances in Thermochemical Conversion of Biomass*, Elsevier Inc., 2015, pp. 383–435. doi: 10.1016/B978-0-444-63289-0.00014-4.

[57] H.-S. Song, D. Ramkrishna, S. Trinh, and H. Wright, “Operating Strategies for Fischer-Tropsch Reactors: A Model-Directed Study,” 2004.

[58] H. Schulz, E. Erich, H. Gorre, and E. van Steen, “REGULARITIES OF SELECTIVITY AS A KEY FOR DISCRIMINATING FT-SURFACE REACTIONS AND FORMATION OF THE DYNAMIC SYSTEM,” 1990.

[59] E. Iglesia, S. L. Soled, J. E. Baumgartner, and S. C. Reyes, “Synthesis and catalytic properties of eggshell cobalt catalysts for the Fischer-Tropsch synthesis,” 1995.

[60] S. M. Kim, J. W. Bae, Y. J. Lee, and K. W. Jun, “Effect of CO2 in the feed stream on the deactivation of Co/γ-Al2O3 Fischer-Tropsch catalyst,” *Catal Commun*, vol. 9, no. 13, pp. 2269–2273, Jul. 2008, doi: 10.1016/j.catcom.2008.05.016.

[61] O. Olsvik and R. Hansen, “High Pressure Autothermal Reforming (HP ATR),” in *Studies in Surface Science and Catalysis*, vol. 119, A. Parmaliana, D. Sanfilippo, F. Frusteri, A. Vaccari, and F. Arena, Eds. Elsevier, 1998, pp. 875–882. doi: https://doi.org/10.1016/S0167-2991(98)80542-9.

[62] J. G. Speight, “Chapter 5 - The Fischer–Tropsch Process,” in *Gasification of Unconventional Feedstocks*, J. G. Speight, Ed. Boston: Gulf Professional Publishing, 2014, pp. 118–134. doi: https://doi.org/10.1016/B978-0-12-799911-1.00005-4.

[63] R. M. Swanson, J. A. Satrio, R. C. Brown, A. Platon, and D. D. Hsu, “Techno-Economic Analysis of Biofuels Production Based on Gasification,” 2010. [Online]. Available: http://www.osti.gov/bridge

[64] K. M. Holmgren, “Investment cost estimates for gasification-based biofuel production systems,” 2221. [Online]. Available: www.ivl.se

[65] I. Hannula, “Hydrogen enhancement potential of synthetic biofuels manufacture in the European context: A techno-economic assessment,” *Energy*, vol. 104, pp. 199–212, Jun. 2016, doi: 10.1016/j.energy.2016.03.119.

[66] Sennai Asmelash Mesfun, “BIOMASS TO LIQUIDS (BTL) VIA FISCHER-TROPSCH A BRIEF REVIEW Biomass to liquids (BtL) via Fischer-Tropsch-a brief review Author: Sennai Asmelash Mesfun-RISE Sweden Prepared with the support of project ETIP-B-SABS2,” 2021.

[67] F. Hildor, H. Leion, C. J. Linderholm, and T. Mattisson, “Steel converter slag as an oxygen carrier for chemical-looping gasification,” *Fuel Processing Technology*, vol. 210, Dec. 2020, doi: 10.1016/j.fuproc.2020.106576.

[68] H. Leion, A. Lyngfelt, M. Johansson, E. Jerndal, and T. Mattisson, “The use of ilmenite as an oxygen carrier in chemical-looping combustion,” *Chemical Engineering Research and Design*, vol. 86, no. 9, pp. 1017–1026, Sep. 2008, doi: 10.1016/j.cherd.2008.03.019.

[69] T. Roshan Kumar, “Process analysis of chemical looping gasification (CLG) of biomass for liquid fuel production with net-negative CO 2 emissions.”

[70] M. Arvidsson, M. Morandin, and S. Harvey, “Biomass gasification-based syngas production for a conventional oxo synthesis plant-process modeling, integration opportunities, and thermodynamic performance,” *Energy and Fuels*, vol. 28, no. 6, pp. 4075–4087, Jun. 2014, doi: 10.1021/ef500366p.

[71] M. Pondini and M. Ebert, “Process synthesis and design of low temperature Fischer-Tropsch crude production from biomass derived syngas.”

[72] J. Isaksson, A. Åsblad, and T. Berntsson, “Pretreatment methods for gasification of biomass and Fischer-Tropsch crude production integrated with a pulp and paper mill,” *Clean Technol Environ Policy*, vol. 16, no. 7, pp. 1393–1402, 2014, doi: 10.1007/s10098-014-0815-7.

[73] S. Rane, O. Borg, E. Rytter, and A. Holmen, “Relation between hydrocarbon selectivity and cobalt particle size for alumina supported cobalt Fischer-Tropsch catalysts,” *Appl Catal A Gen*, vol. 437–438, pp. 10–17, Sep. 2012, doi: 10.1016/j.apcata.2012.06.005.

[74] C. Davidson, E. Newes, A. Schwab, and L. Vimmerstedt, “An Overview of Aviation Fuel Markets for Biofuels Stakeholders,” 2014. [Online]. Available: www.nrel.gov/publications.

[75] SUNIL KUMAR, SHRIKANT NANOTI, and M O GARG, “Maximising the use of process energy,” *https://www.digitalrefining.com/article/1000960/maximising-the-use-of-process-energy*, 2014.

[76] NETL, “CO2 Compression,” 2022. https://netl.doe.gov/coal/carbon-capture/compression#:~:text=Carbon%20dioxide%20(CO2)%20captured,recovery%2C%20or%20CO2%20utilization (accessed Jun. 22, 2022).

[77] IPCC, “CARBON DIOXIDE CAPTURE AND STORAGE,” 2005.

[78] F. Habermeyer, E. Kurkela, S. Maier, and R.-U. Dietrich, “Techno-Economic Analysis of a Flexible Process Concept for the Production of Transport Fuels and Heat from Biomass and Renewable Electricity,” *Front Energy Res*, vol. 9, 2021, [Online]. Available: https://www.frontiersin.org/article/10.3389/fenrg.2021.723774

[79] G. Liu, E. D. Larson, R. H. Williams, T. G. Kreutz, and X. Guo, “Making Fischer-Tropsch fuels and electricity from coal and biomass: Performance and cost analysis,” *Energy and Fuels*, vol. 25, no. 1, pp. 415–437, Jan. 2011, doi: 10.1021/ef101184e.

[80] G. Liu, E. D. Larson, R. H. Williams, T. G. Kreutz, and X. Guo, “Online Supporting Material for Making Fischer-Tropsch Fuels and Electricity from Coal and Biomass: Performance and Cost Analysis.”

[81] T. G. Kreutz, E. D. Larson, G. Liu, and R. H. Williams, “Fischer-Tropsch Fuels from Coal and Biomass.”

[82] I. Hannula, E. Kurkela, and Valtion teknillinen tutkimuskeskus, *Liquid transportation fuels via large-scale fluidised-bed gasification of lignocellulosic biomass*.

[83] S. Heyne and S. Harvey, “Impact of choice of CO2 separation technology on thermo-economic performance of Bio-SNG production processes,” *Int J Energy Res*, vol. 38, no. 3, pp. 299–318, Mar. 2014, doi: 10.1002/er.3038.

[84] F. Franco, R. Anantharaman, O. Bolland, and N. Booth, “DECARBit Project full title: Enabling advanced pre-combustion capture techniques and plants Collaborative large-scale integrating project European best practice guidelines for assessment of CO 2 capture technologies,” Alstom UK, 2011.

[85] T. Roshan Kumar, T. Mattisson, and M. Rydén, “Techno-Economic Assessment of Chemical Looping Gasification of Biomass for Fischer–Tropsch Crude Production with Net-Negative CO_2 Emissions: Part 2,” *Energy & Fuels*, Jun. 2022, doi: 10.1021/acs.energyfuels.2c01184.

[86] A. de Klerk, “Environmentally friendly refining: Fischer–Tropsch versus crude oil,” *Green Chemistry*, vol. 9, no. 6, pp. 560–56, May 2007, doi: 10.1039/b614187k.

[87] “Natural Gas price,” 2020. tradingeconomics.com (accessed Mar. 24, 2020).

[88] “Gasoline and Diesel price.” https://www.globalpetrolprices.com/ (accessed Mar. 21, 2022).

[89] “Jet A fuel price.” IATA.org (accessed Mar. 18, 2022).

[90] “Wax price.” https://paraffinwaxco.com/ (accessed Mar. 21, 2022).

[91] M. Li *et al.*, “Comprehensive Life Cycle Evaluation of Jet Fuel from Biomass Gasification and Fischer-Tropsch Synthesis Based on Environmental and Economic Performances,” *Ind Eng Chem Res*, vol. 58, no. 41, pp. 19179–19188, Oct. 2019, doi: 10.1021/acs.iecr.9b03468.

[92] I. S. Tagomori, P. R. R. Rochedo, and A. Szklo, “Techno-economic and georeferenced analysis of forestry residues-based Fischer-Tropsch diesel with carbon capture in Brazil,” *Biomass Bioenergy*, vol. 123, pp. 134–148, Apr. 2019, doi: 10.1016/j.biombioe.2019.02.018.